CrossMark
← click for updates

Fabrication, biodistribution, and toxicological evaluation of mesoporous silica nanoparticles based on preclinical studies intended for cancer therapy: A review

Muhammad Esa [ID], Sunisa Kaewpaiboon, Teerapol Srichana* [ID]

Department of Pharmaceutical Technology, Faculty of Pharmaceutical Sciences, Drug Delivery System Excellence Center, Prince of Songkla University, Hat Yai, Thailand.

ABSTRACT

Effective delivery of anticancer drugs to tumor sites remains a substantial challenge in cancer treatment. A significant effort has been devoted to delivering anticancer drugs to the intended targets without causing harm to normal body cells. The need to enhance the efficacy and selectivity of chemotherapeutic drugs while minimizing adverse effects on healthy tissues has resulted in increased attention. A mesoporous silica nanoparticle (MSNP) platform is promising due to low toxicity, controlled release profiles, excellent drug loading capacity, and surface modification for targeting. The literature has outlined the synthesis, fabrication, drug loading and release profile, pharmacokinetics, biodistribution, toxicology, and potential outcomes of employing MSNP for anticancer drug delivery. However, the information is dispersed. This review aims to provide a comprehensive examination of the current research on MSNP for efficient drug delivery in cancer therapy based on over 150 preclinical studies up to March 2025. The review highlights the importance of MSNPs in addressing major challenges in targeted drug delivery for cancer therapy and offers a clear summary of the current state of research. This article will serve as an updated and valuable reference for researchers working on MSNP for anticancer drug delivery.

INTRODUCTION

Drug delivery systems play an important role in tackling the challenges associated with conventional cancer treatment. These problems encompass achieving higher precision in targeting tumors [1], overcoming drug resistance [2], improving drug solubility [3], achieving controlled drug release [4], improving penetration through biological barriers [5], and facilitating personalized treatment regimens [6]. Drug delivery systems improve chemotherapy distribution, reduce toxicity to healthy cells, and enhance treatment efficacy [7]. Recent research attempts have been made to use specialized targeting ligands, nanoparticles, and carriers to enhance drug solubility, provide controlled release, and improve drug penetration [8]. One such example is the mesoporous silica nanoparticle (MSNP) platforms, which present promising potential for drug delivery. These nanosystem platforms have a structured porosity layout with both small size and large surface areas, thereby facilitating drug loading and efficient encapsulation of a wide range of drug (cargo) molecules, including chemotherapeutic agents [9]. Multiple studies have reported that these nanosystems protect cargo molecules, extend their circulation time, and protect drugs from premature degradation by physiological systems [10]. Additionally, their stability and ability for surface modification with targeting ligands provide targeted drug delivery of cargo molecules to their intended targets, for example, a tumor, while mitigating off-target effects and leakage instances [11]. These nanosytems can be modified to achieve precise drug release

---

*Corresponding Author

Teerapol Srichana, Department of Pharmaceutical Technology, Faculty of Pharmaceutical Sciences, Drug Delivery System Excellence Center, Prince of Songkla University, Hat Yai, Thailand.
E-mail: teerapol.s @ psu.ac.th

patterns that ensure sustained release profiles while improving therapeutic efficacy and overall therapeutic outcomes compared to conventional drug administration attempts [12]. Various research studies have shown that MSNP nanosytems have the ability to co-deliver multiple drugs with different modes of action simultaneously, thereby achieving combination therapy with enhanced therapeutic benefits [13].

Several studies in the literature have demonstrated the potential of MSNP systems for the delivery of anticancer drugs and reported that they offer enhanced anticancer activity in various *in vitro* and *in vivo* models. These include 5-fluorouracil [14], capecitabine [15], cisplatin [16], coumarin [17], curcumin and quercetin [18,19], cytarabine and daunorubicin [20], doxorubicin [21], doxorubicin and sorafenib [22], docetaxel [23], guanidine and curcumin [24], irinotecan [25], lenvatinib [26], methotrexate [27], paclitaxel [28,29], vinblastine [30], among others. Many reviews have summarized the applications of these nanosytems; however, they often lack a comprehensive overview of findings from clinical studies, the mechanisms of drug release [31], and active/passive targeting strategies [32,33]. Furthermore, three review articles published in 2012, 2019, and 2022 discussed biocompatibility [34], biodistribution and biosafety [35], and toxicity instances [36] of MSNP nanosystems, mainly focusing on passive targeting and conventional strategies to overcome biodistribution and toxicity instances. During the last 5 years, some novel strategies have been introduced, such as multiple surface modifications [37], peptide-based targeting (i.e., arginylglycylaspartic acid) [38], antibody-based targeting (i.e., epidermal growth factor receptor) [39], folate receptor targeting (i.e., chitosan and polydopamine coated) [40], pH-responsive system (i.e., poly-(lactic-*co*-glycolic acid)) [41], magnetic field-guided targeting (i.e., tannic acid–iron network) [42], and enzyme-responsive functionalization (calpain 2) [43]. This review aims to address these gaps by providing a comprehensive compilation of existing preclinical studies published over the past decade. It will offer a detailed exploration of drug release mechanisms and targeting strategies and place a special focus on the toxicological considerations essential for advancing MSNP-based anticancer drug delivery. The ultimate objectives of this review article are to encourage further research in the area of toxicology, to present existing preclinical research findings, and to illustrate the key functions of MSNP as an anticancer drug delivery platform.

MESOPOROUS SILICA NANOPARTICLE

Basic concepts of synthesis methods

The mesoporous structure of SNP features uniform pore size and interconnected pores in a size range of 2–50 nm [44]. MSNP can be synthesized by different methods. The sol-gel, microwave-assisted, and the Stöber methods are commonly used [45]. The synthesis approach for MSNP using the Stöber and sol-gel methods is shown in Fig. 1 [46]. The three primary components that constitute the basis of MSNP include a silica precursor, a surfactant as a structure-directing agent, and a catalyst [47]. Tetraethyl orthosilicate (TEOS) [48], tetra-alkoxysilanes [49], trimethoxyvinylsilane, and sodium meta-silicate are commonly used as silica precursors. In the Stöber technique, the silica precursors are organized, hydrolyzed, and then condensed in the presence of stabilizing agents [50].
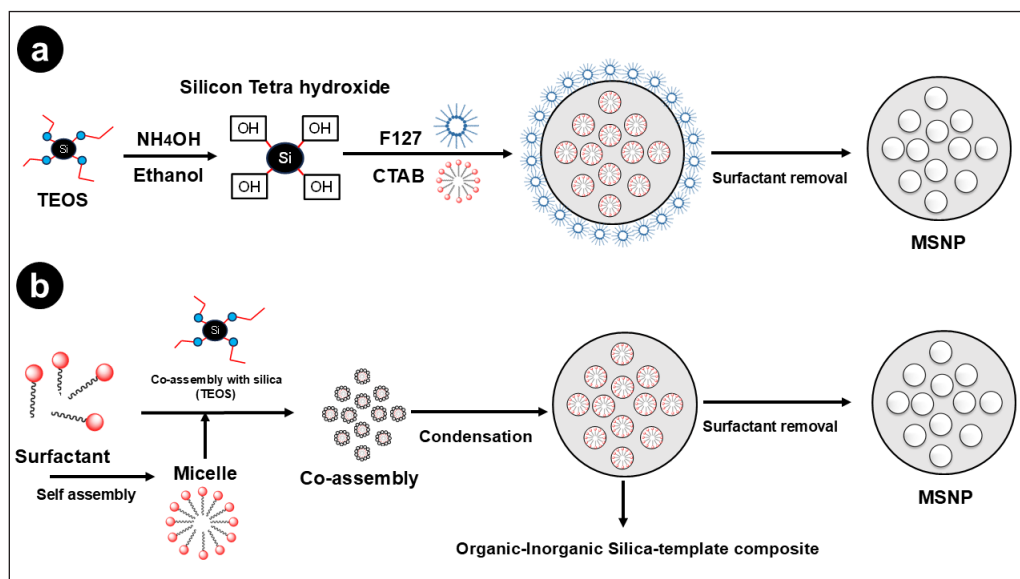

Figure 1. Diagrammatic illustration of MSNP made through different synthesis techniques. In the Stöber method (a),TEOS is hydrolyzed and condensed using ethanol and ammonia as a catalyst, along with surfactant templates CTAB and Pluronic F127 (F127). Si-OH groups are formed when TEOS is hydrolyzed by NH_4OH. These groups then go through condensation processes to generate Si-O-Si bonds, which form the mesoporous structure (b). Micelles are formed through the hydrolysis of a silica precursor, such as TEOS, in the presence of a surfactant, such as CTAB, using the sol-gel process. To produce a mesoporous structure that has a large surface area and pore size, the hydrolyzed silica precursor undergoes polymerization around the surfactant micelles which results in the formation of a silica gel.

Furthermore, the most widely used method involves using either triblock copolymers, such as Pluronic F127 or P123, in strongly acidic conditions, or quaternary alkylammonium surfactants, such as cetyltrimethylammonium bromide (CTAB), as a template, in highly basic conditions [51]. Another approach is template-assisted synthesis, which utilizes templates to create the desired porous nanostructure [52].

Most studies detailing the fabricating of MSNP have focused on the sol-gel method. Hwang *et al.* [53] used sodium silicate and polyethylene glycol (PEG) with a molecular weight of 3,000 g/mole as the silica source and template, respectively. The synthesis process was then carried out in a neutral pH environment using acetic acid as a pH adjuster, ultimately yielding spherical MSNP obtained with a surface area of 685 m^2g^{-1} [53]. In another research effort, Lv *et al.* [54] attempted to produce an MSNP nanosystem using TEOS as the template, CTAC as the silica source, and tetraethylammonium as a catalyst in slightly basic conditions [54]. Additionally, Zhou *et al.* [55] used CTAB as a template, silica fume as the silica supply, and ethyl acetate as a catalyst to effectively produce MSNP. They characterized the resulting nanosystems through X-ray diffraction analysis (XRD), which revealed a hexagonal pore structure of MSNP that presented a peak at 2.2 [55].

Recently, an innovative method to produce MSNP, referred to as the "green method," has received a great deal of attention as an alternative to conventional synthesis approaches. The word "green" indicates that the technique is eco-friendly and can be put forward utilizing waste as the primary source of silica. However, while this approach is considered eco-friendly, it may not always adhere to the principles of green chemistry. For example, the procedure of obtaining sodium silicate, which is a silica source, from waste substances such as rice husk ash requires the use of highly acidic or highly alkaline conditions. Abburi *et al.* [56] successfully produced MSNP without using a template and employed hexafluorosilicic acid, a byproduct of the fertilizer industry, as the source of silica. The XRD data demonstrated that the resulting MSNP possessed a well-organized and hexagonal mesoporous configuration [56]. Furthermore, Mohamad *et al.* [57] attempted to utilize banana peel ash and CTAB as the silica source and template to synthesize MSNP [57]. Similarly, Li and colleagues employed TEOS as a silica source and utilized a modified amino acid as a template to develop MSNP. Transmission electron microscopy images revealed that the MSNP exhibited pores arranged in a "wormhole" pattern. The resulting MSNP had a surface area within the range of 239–678 m^2g^{-1}, while the particle size ranged from 130–270 nm [58].

Formation mechanisms

The formation of MSNPs is achieved through two main techniques: sol-gel chemistry and template-assisted synthesis. Both methods include the use of fundamental processes such as hydrolysis, condensation, and silica precursor elimination, ultimately leading to the formation of the desired porous structure [59]. In the sol-gel method, silica precursors, such as alkoxysilanes (commonly TEOS, TMOS, and TEVS), undergo hydrolysis and condensation. Alkoxysilanes react with water in the presence of a catalyst (acidic or basic) during hydrolysis,

therefore breaking the alkoxy linkages and generating silanol groups. These silanol groups then undergo condensation, where they link together, forming a three-dimensional silica network. This network serves as the basic structure of the MSNP [60]. A preclinical study reported efficient synthesis of MSNPs with a size ranging from 35 to 39 nm using by sol-gel method [61]. Similarly, MSNPs were synthesized using CTAB as a surfactant, sodium dodecyl sulfate as a structure-directing agent, and TEVS as a silane coupling agent through the sol-gel method. The resulting MSNPs (28–34 nm) were loaded with doxorubicin, and surface functionalized with vinyl acrylic acid and n-isopropyl acrylamide, which exhibited dual-responsive (temperature and pH) release and enhanced anticancer activity against HFF-2 and MCF-7 cell lines [62]. A study attempted to synthesize MSNP using hexadecyltrimethylammonium bromide as surfactant and tetraethyl orthosilicate as silica precursor sol-gel method. The resulting nanosystem was loaded with tin, and functionalized with mercaptopropyltriethoxysilane ligand triphenylstannyl resulting in enhanced selective toxicity toward breast cancer cells *in vitro* and *in vivo* (BALB/c mice) [63].

Using either organic or inorganic templates, the template-assisted synthesis approach guides the formation of pores inside the silica structure. Under this method, combined with the precursor solution, templates such as block copolymers or surfactants self-assemble into structures such as micelles or vesicles. These organic templates produce the required pores by forming spaces inside the silica structure upon the template removal and condensation of the surrounding silica [64]. Organic templates can create various shapes such as arrays, vesicles, or micelles, offering flexibility in the design of the mesoporous structure and are particularly useful for creating MSNP with controlled pore sizes [65]. Inorganic templates, such as silica nanoparticles [66], and colloidal crystals [67], are commonly used. Silica nanoparticles form a protective framework around which the precursor condenses, creating a mesoporous structure [66]. Periodic configurations of nanoparticles called colloidal crystals let the precursor pass between particles to form a continuous silica matrix [68]. The resultant structure appears organized and mesoporous after the removal of the template. This approach provides excellent control over the internal structure and organization of the MSNP [66,67]. A previous study reported the synthesis of MSNP (140–600 nm) for loading cabazitaxel using Pluronic F127 and CTAB as soft templates to form the core and the shell [69]. Another study reported efficient synthesis of MSNPs (20–60 nm) using PEG as a template and CTAC as a structure-directing agent from a sodium silicate solution [70].

Surface functionalization

After synthesizing MSNP, surface engineering and functionalization approaches can be applied to customize its properties for specific biomedical applications. These modifications enhance biocompatibility, stability, targeting efficiency, and drug loading capabilities. Silane coupling agents are commonly used to introduce functional groups, such as amino ($-NH_2$), thiol ($-SH$), carboxyl ($-COOH$), or hydroxyl ($-OH$), onto the MSNP surface. These modifications improve drug loading, targeting, and dispersion in biological

environments [71]. It has been established that coating MSNP with polymers, such as PEG or polyethyleneimine, can enhance the stability and provide a platform for further functionalization [72]. Functionalization methods include click chemistry, which enables the attachment of specific molecules through azide–alkyne cycloaddition with high specificity and efficiency [73]. Biomolecules, such as peptides or antibodies, can be attached to the surfaces through bioconjugation that enables specific interactions enabling targeted drug delivery and cell-specific interactions. It is possible to modify the surface charge by attaching charged molecules or polymers, which results in influencing MSNP's interaction with biological membranes and improving cellular uptake [74].

Stimuli-responsive functionalization involves incorporating functional groups responsive to specific conditions including internal stimuli such as pH, redox reactions, and enzymes, as well as external stimuli such as an alternating magnetic field, ultrasound, and visible light [75]. Layer-by-layer assembly was described by Li *et al.* [76] in which alternating layers of oppositely charged molecules were adsorbed onto the surface. Additionally, host–guest interactions that employ cyclodextrins to encapsulate guest molecules are further techniques for the surface engineering of MSNPs to encapsulate anticancer drugs [76]. Furthermore, Wei *et al.* [77] used biomimetic functionalization (utilized polydopamine coating) to immobilize biomolecules on the MSNP surface to mimic particular biological interactions. According to Zoppe *et al.* [78], surface-initiated polymerization permits the direct formation of polymer chains from the MSNP surface. This technique allows control over the polymer structure and the capacity to precisely affect and design the arrangement of the polymer chains on the MSNP surface [78]. Lastly, antibodies, aptamers, cell membranes, gatekeepers, and vitamins are some of the choices of functionalization schemes that depend upon the desired application and specific requirements (Fig. 2) [79].

DRUG LOADING AND RELEASE PATTERNS

Drug loading methods

An MSNP carrier offers the ability to encapsulate both hydrophilic and hydrophobic drugs within its mesoporous structure. Different loading techniques can be employed based on the solubility of the drugs and their compatibility with the MSNP surface [80]. These loading techniques include incubation, co-precipitation, solvent evaporation, electrospinning, and impregnation methods. Particularly, hydrophilic drugs can be loaded via the incubation method by immersing MSNP in a drug solution, whereas hydrophobic drugs can be co-precipitated with a silica precursor during synthesis, which is termed the "co-precipitation method" [81]. Hydrophobic drugs can also be dissolved in an organic solvent along with the MSNP particles and then evaporated, which is called the solvent evaporation method. On the other hand, hydrophobic drugs can be physically adsorbed onto the MSPN surface, using the impregnation method [82].

Factors affecting drug loading

Specifically, some preclinical studies have studied the effects of surface functionalization on loading anticancer drugs onto an MSPN carrier. As an example, the loading of cisplatin [83] or mitoxantrone [84] increased by multiple folds (almost 16% weight for cisplatin and 18% w/w for mitoxantrone), upon the insertion of sulfhydryl groups (–SH). Similarly, after functionalizing the particles with a carboxylic group (–COOH) or phosphate groups (–PO_4^{3-}), Chang *et al.* [85] found that doxorubicin loading in MSNP improved with a loading content of 31.0%, and entrapment efficiency of 89%, in comparison to non-functionalized MSNP (loading content of 5.8%, and entrapment efficiency of 12.4%). The loading of paclitaxel into MSNPs was not improved by the insertion of carboxylic groups or phosphate groups [85]. Additionally,
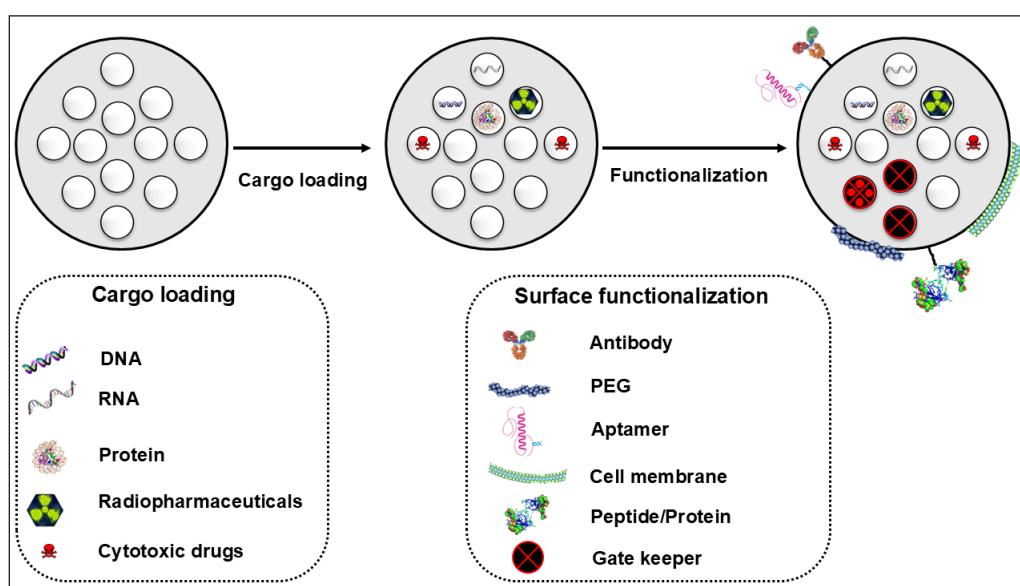

Figure 2. Schematic representation of cargo loading and surface functionalization options of MSNP to enhance selectivity and modify drug release patterns.

She *et al.* [86] concluded that the maximum loading of 5-fluorouracil (5-FU) in MSNPs was achieved through functionalization with amino or cyano groups. With amino and cyano groups functionalization, the loading content was 28.89% and 22.54% in contrast to non-functionalized MSNPs (18.34%) [86]. Furthermore, Bahrami *et al.* [87] concluded that modifying MSNP with a carboxylic acid derivative of piperazine increased the amount of gemcitabine loaded into the nanosystem. The loading content and entrapment efficiency were 35.61% and 55.30% for functionalized MSNPs, compared to 7% and 7.9% for non-functionalized MSNPs [87].

Another strategy is mesopore engineering, which involves adjusting the size, morphology, and surface properties of the mesopores within the MSNPs. By adjusting the pore size and surface area, drug diffusion into the mesopores can be optimized, which leads to improved drug loading efficiency [88]. Additionally, Yang *et al.* [89] concluded that fabricating MSNPs with a core–shell structure can enhance loading efficiency by providing additional space for drug encapsulation. To achieve core–shell structure, they mixed doxorubicin-loaded MSNP suspension with $FeCl_3$, $AlCl_3$, and tannic acid solution under ultrasonication. Doxorubicin loading content and entrapment efficiency increased from 10.3 and 44.2% to 15.7 and 68.2%, respectively [89]. The use of external variables such as magnetic field impacts the drug loading into the MSNPs. These stimuli have the potential to increase drug loading efficiency and boost the overall efficacy of MSNPs as a drug delivery system. For instance, breviscapine loading content significantly increased from 5.12% to 8.63% ($p \leq 0.05$) by employing ultrasound-assisted drug loading [90].

Strategies for drug release

MSNP systems possess the advantage of precise and responsive drug release that makes them ideal for targeted and prolonged drug administration. Multiple strategies can be utilized to induce regulated drug release from the nanosystem, such as active and passive drug release. Surface contact, pH sensitivity, and concentration gradients all affect the spontaneous diffusion of drugs from nanopores, which is the primary mechanism behind passive drug release from MSNPs. Although the passive process provides a steady release of cargo over time, it lacks precise control. To accomplish targeted and controlled drug delivery, active drug release employs internal or external stimuli [91].

Stimuli-responsive drug release

MSNPs provide the benefit of controlled drug release, which can be triggered by internal stimuli such as pH, redox reactions, and enzymes, as well as external stimuli such as alternating magnetic fields, ultrasound, and visible and near infra-red light (Fig. 3). Diffusion-controlled release refers to the slow movement of drug molecules out of the mesopores, which results in sustained release over a prolonged duration. A pH-responsive release can be accomplished by integrating pH-sensitive linkers or coatings to enable medication release in response to pH alterations, such as the acidic tumor microenvironment [92]. For instance, Guo *et al.* [93] utilized a temperature-responsive release strategy and coated temperature and H_2O_2-sensitive nanovalves onto the MSNP carrier to trigger drug release upon exposure to specific temperatures (37°C and above), such as hyperthermic conditions (42°C). The Bhaskar and Korsmeyer-Peppas models showed R^2 values of 0.960, 0.941, 0.985, and 0.996 in H_2O_2 (0.1 and 0.2%) and temperature (37°C and 42°C), respectively. The R^2 values higher than 0.960 in the release medium of 37°C and 42°C demonstrate that the thermoresponsive controlled release is suitable for both kinetic models [93].

Enzyme-responsive release involves functionalizing MSNP with enzyme-responsive moieties that undergo specific cleavage or degradation in the presence of overexpressed enzymes, which results in targeted drug release [94]. Moreover, the magnetic-responsive release takes advantage of MSNP loaded with magnetic nanoparticles, which can be triggered to release drugs in response to an external magnetic field. An MSNP nanosystem showed controlled drug release efficiency (67%) by employing an external magnetic field for a short period (5 minutes), showing faster and higher drug desorption [95]. Additionally, Lu *et al.* [96] used multiple stimulus combinations of pH, redox, and near-infrared (NIR) radiation-responsive drug delivery systems to provide more sophisticated and controlled drug release profiles from an MSNP carrier. The cumulative release amounts of doxorubicin at pH 5.0 (PBS) were higher than those at pH 7.4 (PBS). Additionally, the maximized cumulative release was 50.3% under the condition of pH 5.0 (PBS), GSH, and NIR irradiation. It was 1.52- and 2.23-fold higher compared to the release amount under the single condition of GSH (33%) or NIR irradiation (22.6%), implying that the nanosystem had pH/NIR/redox stimuli-responsive drug release properties [96]. Li *et al.* [97] attempted to attach the folate component to polyethylenimine by forming an amide bond on the surface of the doxorubicin-loaded MSNP to specifically target tumors that are folate-dependent. This method exhibited a loading efficiency of 12.3% with a pH-dependent release behavior (higher at pH 4.7 than at pH 7.4). The study showed encouraging outcomes in terms of enhanced anti-tumor efficacy as evidenced by its
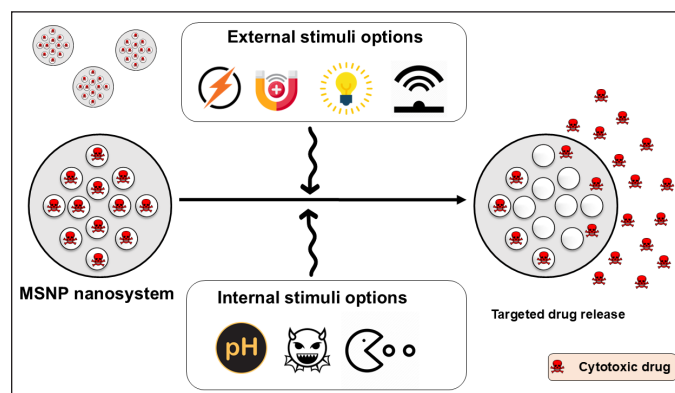

Figure 3. MSNPs provide the benefit of controlled and responsive drug delivery, which can be triggered by internal stimuli such as pH, redox reactions, and enzymes, as well as external stimuli such as alternating magnetic fields (AM Field), ultrasound (US), and visible (Vis) and near infra-red light.

high capacity to be absorbed by cells and its ability to induce cell death in both human breast cancer cells (HUVEC) and cervical cell lines (HeLa), surpassing the performance of non-targeted nanocarriers [97].

Strategies for controlling drug release from MSNP

Wang *et al.* [98] attached nanovalves to the MSNP surface using cyclodextrin and benzimidazole modification. The prepared benzimidazole-modified cyclodextrin nanovalve blocked the mesopores in neutral conditions. The payload (loaded drug; *p*-coumaric acid) was released through pores and nanovalves due to a significant reduction in the binding constant between benzimidazole and benzimidazole-cyclodextrin combination under acidic circumstances. This caused the benzimidazole molecules to be expelled [98]. Du *et al.* [99] conducted an additional study where they utilized p-anisidine linkers and α-cyclodextrin rings to develop a pH-sensitive nanovalve that may be used to encapsulate MSNP in a biocompatible manner. The study findings indicated that drug leakage was not observed at the normal pH level (~7.4), and the pH-sensitive nanosystem demonstrated exceptional stability in biological conditions. Moreover, when the pH was around 5.5 (the pH of lysosomes), maximum drug release (~95%) occurred due to the protonation of para-anisidino nitrogen atoms [99]. Chen *et al.* [100] created an MSNP-based drug delivery system loaded with doxorubicin that responded to changes in pH that targeted both the acidic lysosomal compartments of cancer cells and the slightly acidic tumor microenvironment. Initially, the MSNP carrier was coated with mono-6-deoxy-6-EDA-β-CD and then degraded at pH 5 using a pH-sensitive boronate ester bond. Likewise, a pH-responsive benzoic imine linkage that underwent degradation at pH 6.5 was employed to transfer PEG from the particles. The presence of PEG moieties enhanced the internalization of the nanoparticles by cells under acidic pH conditions. pH-sensitive bonds were progressively broken resulted in the release of payloads within the tumor cells in a synergistic fashion [100].

Eskandari *et al.* [101] described a gold nanoparticle biotin-capped MSNP anticancer delivery system that utilized a peptide-cleavable linker responsive to matrix metalloproteinases (MMPs). The study findings demonstrated that the drug-loaded nanocarrier effectively caused cell death in the MMP-2 overexpressed cell lines during *in vitro* experiments [101]. Mondragón *et al.* [102] employed protease-cleavable poly-L-lysine molecules to seal the camptothecin-loaded MSNP. Drug release studies showed a nearly zero cargo release in water due to the coverage of the nanoparticle surface by polymer ε-poly-L-lysine, while 69%–91% of the drug release was achieved within 6 hours after protease addition. Furthermore, treatment with camptothecin-loaded MSNPs led to an ~85% decrease in the viability of human cervical epithelial carcinoma (KB-V1) cells, even at the lowest concentration (50 mg/ml) [102]. Another study involved the development of highly organized hexagonal MSNPs loaded with etoposide. The MSNP carrier was functionalized with amino groups to assess the effect of amine functionalization on the release behavior of the MSNP nanosystem. The release patterns of crystalline etoposide, commercial formulation, etoposide-MSNP, and etoposide-MSNP-amino were assessed and compared by the researchers. The drug release rate from etoposide-MSNP-amino was considerably higher in comparison to both commercial formulations and crystalline etoposide. The observed results were attributed to the quicker dissolution rate of etoposide from etoposide-MSNP-amino, which was roughly 5.1 times faster than crystalline etoposide and 1.16 times faster than the commercial formulation [103].
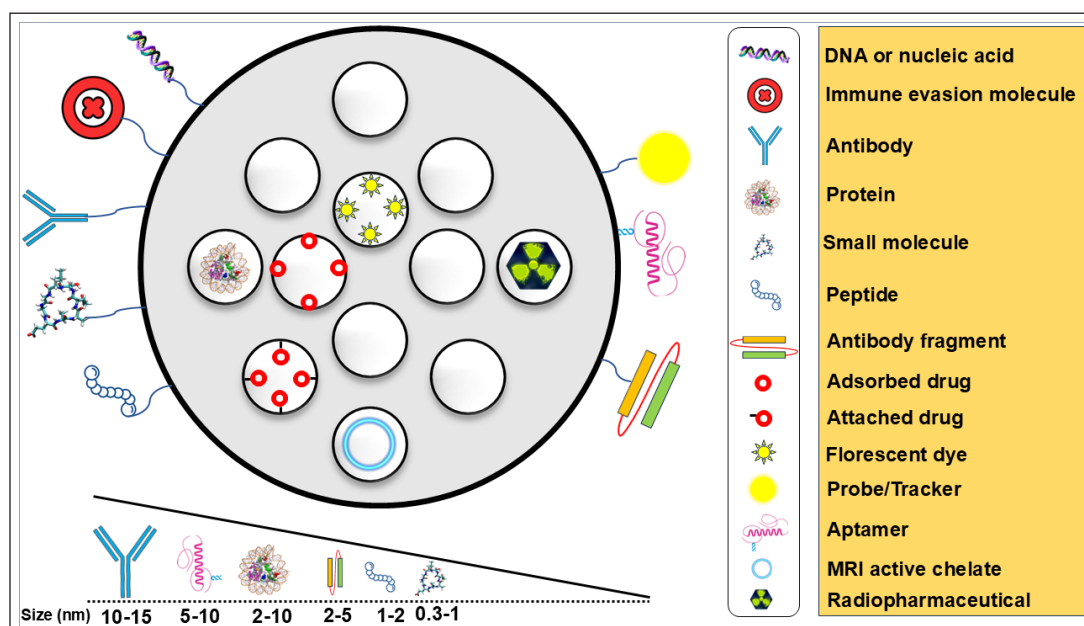

Figure 4. Surface decoration possibilities offered by MSNP to promote biocompatibility and controlled and on-demand drug delivery. Targeting moieties and their sizes are also summarized.

APPLICATION OF MSNP IN ANTICANCER DRUG DELIVERY

Targeted drug delivery systems

Targeted drug delivery is a strategy designed to increase the concentration and effectiveness of drugs at specific sites, such as tumors, while reducing unintended side effects thereby preventing therapy-related issues such as anemia, hair fall, and gastric problems. Active and passive targeting are the two frequently employed techniques for targeted drug delivery employing MSNP [94]. Active targeting refers to the process of modifying MSNP carriers with ligands that can selectively bind to receptors that are excessively expressed on the outer surface of specific target cells [104]. As mentioned earlier, multiple studies have attempted to attach different types of ligands onto the surface of MSNP, which include antibodies [105], peptides [106], aptamers [107], or small molecules that have high affinity and selectivity for the target receptors [108]. Various surface decoration possibilities offered by MSNP carriers to promote controlled and on-demand drug delivery are depicted in Fig. 4 [109].

Once these ligands are added to the MSNP, they may effectively attach to the target cells to facilitate receptor-mediated endocytosis and internalization of MSNP into the target cells. Thus, it can enhance the drug delivery system to the specified cell population. Active targeting enhances the specificity and effectiveness of drug delivery to enable accurate targeted therapy [110]. On the other hand, a passive targeting strategy exploits the unique aspects of the tumor microenvironment. Tumors frequently display a vasculature that is permeable and lymphatic drainage that is compromised, which leads to enhanced vascular permeability. This phenomenon is known as the enhanced permeability and retention (EPR) effect. MSNP carriers can permeate blood arteries and selectively aggregate within tumor tissues due to their tiny size and distinctive surface characteristics. The EPR effect enables the passive accumulation of MSNP specifically at the tumor site, hence improving the movement of drugs to the tumor tissues [111]. Surface functionalization of MSNP with specific ligands is essential to allow active targeting and enhance the selectivity, and the uptake of MSNP into the desired sites such as tumor tissues. A few examples are listed in Table 1.

Preclinical studies

Rivero-Buceta *et al.* [122] developed a stable conjugated ligand of doxorubicin by utilizing an anti-prostate-specific membrane antigen molecule (anti-FOLH1 monoclonal antibody, clone C803 N) in MSNP, targeting androgen-independent prostatic carcinoma. This novel drug delivery approach showed improved cell internalization by approximately 25% in physiological conditions during experimental testing. In comparison to untargeted MSNP and free drugs, doxorubicin cytotoxicity increased two-fold [122]. Kumar *et al.* [123] developed an enzyme-responsive system to boost the efficacy of 5-FU as a colon cancer treatment utilizing MCM-41-type as a mesoporous material. Guar gum, a naturally occurring polymer, was used to functionalize MSNP to retain 5-FU within the mesoporous channels under normal physiological conditions. The breakdown of the guar gum cap inside the intestine, triggered by colonic enzymatic activity, led to the release of 5-FU. In the absence of enzymes in different gastrointestinal tract conditions, almost no release occurred. This study highlighted the potential of MSNP as an effective *in vivo* enzyme-responsive carrier using guar gum capping [123].

Another study demonstrated enhanced delivery of paclitaxel and doxorubicin to malignant brain glioma using protein-grafted MSNP. The outer surface of MSNP was functionalized with transferrin, a glycoprotein found in blood, along with a magnetic silica poly (D, L-lactic-co-glycolic acid) nanosystem. Transferrin acted as both a gatekeeper

Table 1. Surface functionalized MSNP systems explored for tumor targeting.

Cargo	Drug	Anticancer drug class	Targeting Ligand	Receptor	Application	References
Surface functionalized MSNP	5-FU	Antimetabolite	EGF	EGF	Colorectal cancer	[112]
	5-FU	Antimetabolite	Hyaluronic acid	CD44	Colorectal cancer	[113]
	Curcumin	Polyphenol	Chondroitin sulfate	CD44	Cervical cancer	[114]
	Doxorubicin	Anthracycline	Aptamer	EpCAM	Colon cancer	[115]
	Doxorubicin	Anthracycline	Transferrin	Transferrin	Hepatic cancer	[116]
	Docetaxel	Taxane	Folic acid	Folate	Breast cancer	[117]
	Docetaxel	Taxane	Lactose	Asialoglycoprotein	Hepatoma	[118]
	Quercetin	Flavonoid	Folic acid	Folate	Breast cancer	[119]
	Quercetin	Flavonoid	cRGD peptide	Integrin receptor αvβ3	Triple negative breast cancer	[120]
	Sunitinib	Tyrosine kinase inhibitor	VEGF121	VEGF	Glioblastoma	[121]
	Topotecan	Topoisomerase inhibitor	cRGD peptide	Integrin receptor αvβ3	Triple-negative breast cancer	[120]

Abbreviations: 5-FU: 5-fluorouracil; EGF: Epidermal growth factor; VEGF: Vascular endothelial growth factor; EpCAM: Epithelial cell adhesion molecule; cRGD: Cyclic arginine-glycine-aspartic acid

and targeting agent, enhancing the therapeutic efficacy of doxorubicin. The study reported drug loading and entrapment efficiency for paclitaxel at 136.4 ± 2.1 µg/mg and $89.2\% \pm 1.1\%$ and doxorubicin at 31.3 ± 2.8 µg/mg and $22.0\% \pm 0.8\%$, respectively. Additionally, the presence of a magnetic field resulted in increased cytotoxicity of doxorubicin ($IC_{50} = 0.52$ µg/ml, ~8.6-fold higher than free drug combination) and an accelerated release rate (24 hours, ~19% for doxorubicin and 57% for paclitaxel) compared to unbound doxorubicin. These treatments resulted in a 47.5-fold reduction in tumor size after 20 days compared to the free drug combination. This transferrin-modified MSNP carrier holds great potential for inhibiting tumor growth and delivering targeted cytotoxic effects against glioblastoma while minimizing systemic side effects [124]. Mo *et al.* [125] modified the size of MSNP to effectively penetrate the BBB and specifically target glioblastoma. MSNP carriers can be produced in various sizes (20, 40, and 80 nm) and coated with a peptide called arginylglycylaspartic acid coupled with doxorubicin. These MSNP carriers possessed stronger permeability across the BBB and specifically bind to a human glioblastoma cell line (U87 cells) that expressed a significant amount of integrin that led to enhanced cellular uptake. This was achieved by using 40 nm particles. The IC_{50} of doxorubicin-loaded MSNP carriers (3.31 nM) against U87 cells was about 60 times lower than that of free drug (197.51 nM). Therefore, modifying the size and functionalization of MSNP carriers may be a promising strategy to specifically target glioblastoma by successively enhancing the cancer-targeting impact [125].

For treating hepatocellular carcinoma, Chi *et al.* [126] encapsulated arsenic trioxide prodrugs within the mesopores of MSNP. When magnetic iron oxide nanoparticles are incorporated into the MSNP pores, this system can be used with real-time monitoring using magnetic resonance imaging. By employing a folic acid ligand to modify the silica surface, stimuli-responsive targeting was accomplished. Due to a notable activation of death in the human hepatoma SMMC-7721 cell line, folic acid-functionalized MSNP demonstrated enhanced cytotoxicity efficacy with an IC_{50} value of 0.36 µM compared to free drug IC50 = 13.75 µM after 48 hours . Additionally, the produced nanocarrier of imaging capability *in vivo* demonstrated a targeted and controlled release behavior with 80% drug release at pH 5.4 (resembling tumor microenvironment pH) while only 13% drug release at pH 7.4 [126]. Liu *et al.* [127] successfully fabricated biocompatible core–shell-constructed MSNP that efficiently promoted tumor apoptosis in prostate cancer cells (LNCaP-AI cells). The potential of a doxorubicin-loaded MSNP nanosystem capped with calcium carbonate presented penetration and accumulation in high concentrations at the tumor site by coating them with a malignant cell membrane layer. The surface of the nanocarrier was modified to include a detachable pH-sensitive stimulus, which allowed for the controlled release of doxorubicin without altering the shape of the nanosystem. These formulations of doxorubicin exhibited enhanced anticancer activity when discharged in an acidic environment (pH 6.5 and 5.0) compared to its uncharged state. After 48 hours, at pH 7.4, only 2.7% drug was released while with a further decrease in pH (pH 6.5), drug release slightly increased to above 20% (8 hours of incubation). The highest drug release rate was observed at pH 5.0 and nearly 70% of encapsulated drug was found to release. The formulation was non-cytotoxic to normal liver cell line QSG-7701, and no hemolysis was reported in erythrocyte
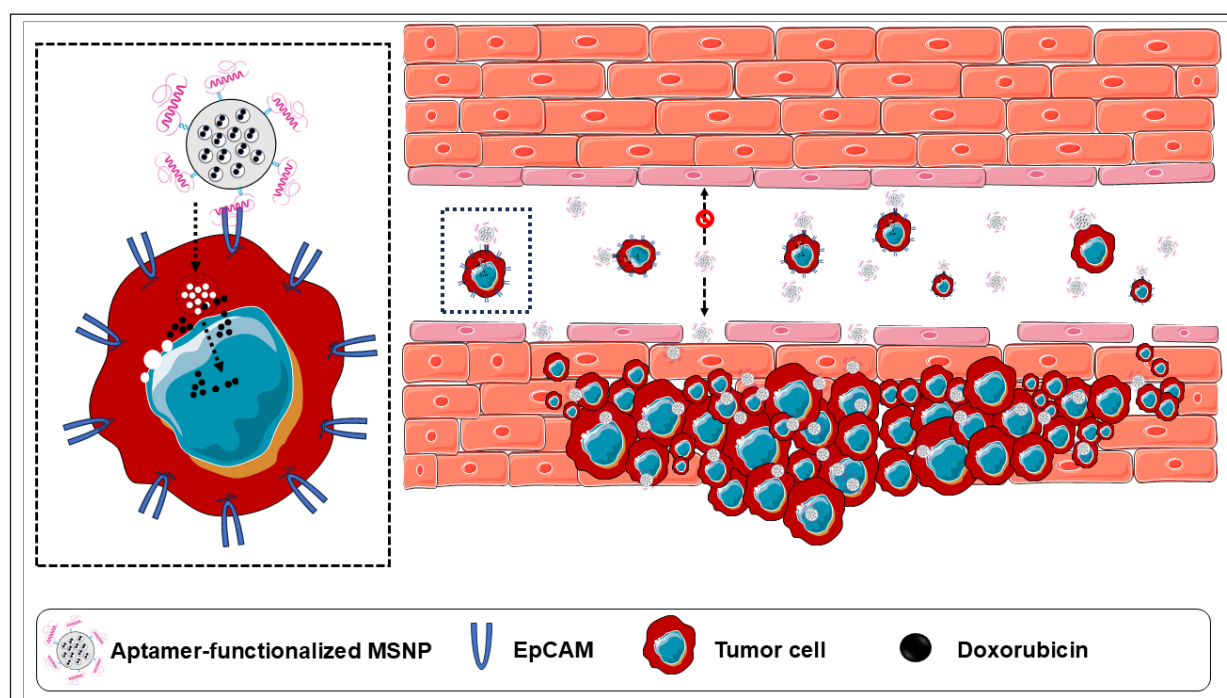

Figure 5. Epithelial cell adhesion molecule (EpCAM) aptamer-functionalized MSNP for effective and targeted drug delivery of doxorubicin in colon cancer. A preclinical study based on the hypothesis mentioned in the figure can be found in reference [115].

cells. Lastly, the average tumor weight in BALB/c nude mice MSNP treated group significantly ($p < 0.001$) reduced by 71% compared with the free doxorubicin (5 mg/kg) treated group (38%) [127]. From previous preclinical studies, MSNP carriers were functionalized with aptamers, which are single-stranded DNA or RNA molecules, to facilitate targeted drug delivery by specifically binding to their target molecules on the surface of cancer cells (Fig. 5) [128].

Overcoming biological barriers

Understanding the biodistribution and pharmacokinetics of MSNP carriers is essential to enhance their effectiveness [129]. Cellular internalization of MSNP can occur through endocytosis and receptor-mediated uptake. Once inside the tumor cells, MSNP can release their cargo, thereby enabling the drug to exert its therapeutic effect. Additionally, it also protects the cargo from degradation and enhances its intracellular bioavailability [130]. Upon administration, MSNP carriers engage with biomolecules found in biological fluids, which results in the formation of a protein core on their surface. The distribution of MSNP in cells is affected by various parameters that include particle size, surface charge, and modifications [131]. After administration, MSNP can be taken up by macrophages in organs such as the liver and spleen, which play a role in clearing foreign materials from the body [132]. The fate of MSNP can also be influenced by biodegradability. Some MSNP carriers are designed to degrade gradually, either releasing entrapped drugs over time or breaking down into

smaller fragments that can be eliminated more easily [35]. According to Ahmadi *et al.* [133], smaller MSNP carriers have a higher probability of reaching the target tissues due to their improved ability to leak out from blood vessels through the EPR effect.

To achieve effective tumor penetration, MSNP can be engineered with specific surface modifications or coatings. These modifications can enhance the interaction of MSNP with tumor cells, thereby promoting their uptake [134]. For instance, targeting ligands can be attached to the surface of MSNP carriers to recognize and bind to receptors that are overexpressed on tumor cells, such as folate receptors. For instance, the influence of folate receptor expression on the cellular absorption of functionalized MSNP was demonstrated in research by Heidari *et al.* [135]. They used MSNP functionalized with PEG and folic acid to treat HeLa-RDB cells, which are known to have high folate receptor expression, and EPG85.257-RDB cells, which have low folate receptor expression. The findings highlighted the function of folate conjugation in boosting cellular absorption in cells with high numbers of folate receptors by demonstrating that HeLa-RDB cells internalized functionalized MSNP noticeably more efficiently than non-functionalized. On the other hand, because of their poor expression of the folate receptor, EPG85.257-RDB cells demonstrated limited internalization of the functionalized MSNP. The specificity of folate-receptor-mediated endocytosis was confirmed by further experiments that showed that the introduction of extra free folates impeded the absorption of functionalized MSNP by
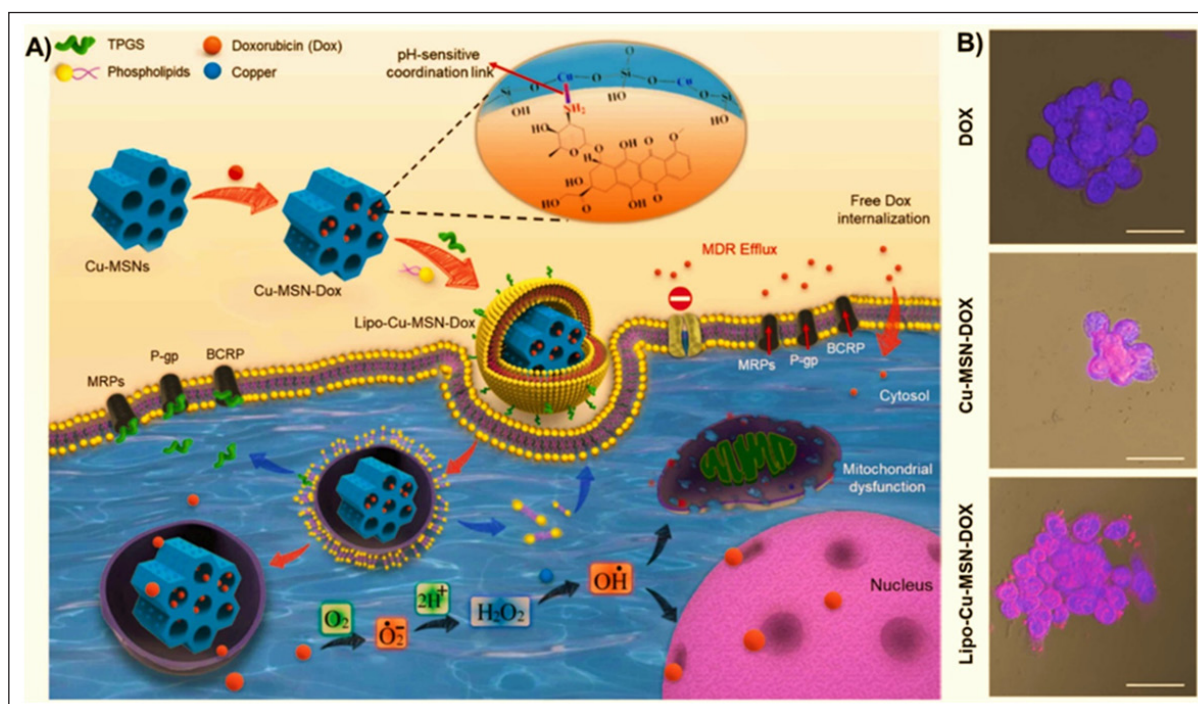

Figure 6. (A) The process of synthesis and cell internalization of MSNPs loaded with doxorubicin (DOX) and the mechanism of overcoming multi-drug resistance (MDR). (B) Confocal microscopy observations demonstrate the cellular uptake of different nanocarriers, specifically copper-substituted MSNP loaded with doxorubicin (Cu-MSN-DOX) and liposome-coated MSNP loaded with doxorubicin (Lipo-Cu-MSN-DOX) at a concentration of 20 µg/ml compared to pure doxorubicin at a concentration of 5 µg/ml in a human uterine sarcoma doxorubicin-resistant tumor (MES-SA/Dx-5 resistant cell line). Reprinted with permission from [140].

HeLa-RDB cells [135,136]. This targeted approach increases the probability of internalization by cancer cells and reduces non-specific interactions with healthier tissues or non-cancerous cells [137].

In addition, MSNP carriers can deliver drugs to the brain and cross the BBB. For instance, Zhu *et al.* [138] concluded that a surface-modified MSNP carrier loaded with paclitaxel was able to cross the BBB and supply the chemotherapeutic drug to glioma cells. Pharmacokinetic studies demonstrated that only 2.49% of free drugs crossed the BBB and the MSNP-loaded drug (2.72%), indicating a negligible improvement achieved by MSNP entrapment. However, surface-modification with lipid coating and angiopep-2 significantly increased the transport ratio across the BBB (10.74%) [138].

Efflux pumps and multidrug resistance (MDR) pose significant challenges in cancer treatment. Efflux pumps, such as ATP-binding cassette (ABC) transporters, actively propel drugs out of the tumor cells to prevent intracellular accumulation and reduce their efficacy [139]. MSNP carriers offer potential solutions for overcoming these issues. After MSNP carriers are loaded with anticancer drugs, they can shield efflux pumps or inhibit their activity (Fig. 6). The study demonstrated that doxorubicin loaded into copper-substituted MSNP and liposome-coated MSNP can shield efflux pumps and inhibit their activity, even at very low concentrations, with IC_{50} values of 3.5 and 1.8 μg/ml, in contrast to pure doxorubicin (IC_{50}=22.7 μg/ml). Additionally, confocal microscopy studies demonstrated that liposome-coated MSNP exhibited significant uptake in the human uterine sarcoma doxorubicin-resistant tumor (MES-SA/Dx-5 resistant cell line), compared to the free drug molecules [140].

Cytotoxic drugs can be encapsulated within the MSNP to reduce their interaction with efflux pumps, which can lead to enhanced intracellular accumulation and improved therapeutic efficacy [134]. Furthermore, MSNP carriers can be engineered to modify other cellular processes associated with MDR. For example, the co-delivery of chemotherapeutic drugs and MDR modulators within MSNP can sensitize cancer cells to chemotherapy and overcome MDR. Fang *et al.* [141] focused on developing an enhanced chemotherapy treatment for gastric carcinoma (GC) by utilizing hyaluronic acid (HA)-modified MSNP to deliver both quercetin and doxorubicin. The HA modification was aimed specifically at the overabundance of CD44 receptors, which are HA receptors on GC cells. Simultaneous administration of quercetin and doxorubicin was observed to enhance the efficacy of GC treatment. Furthermore, this strategy showed relevance to overcoming challenges such as the tumor microenvironment and MDR. The results of quercetin and doxorubicin-loaded HA-MSNP demonstrated excellent stability in physiological pH and sustained release characteristics in an acidic medium, with only 30% of drug release at pH 7.4 (48 hours), while more than 80% of the drug release at pH 5.0 (48 hours). This resulted in improved effectiveness in both *in vitro* and *in vivo* studies compared with individual delivery methods [141].

In addition to the above approaches, the process of cloaking MSNP carriers with cell membranes offered advantages in terms of resisting immune clearance and extending the duration of blood circulation for the nanosystem. Red blood cells (RBCs) circulate in the blood for around 120 days before elimination by macrophages. They possess several self-markers such as CD47 proteins, acidic sialyl moieties, and glycans on their surface that enable them to evade immune responses. Therefore, the process of modifying MSNP with RBC membranes can enhance their biocompatibility and allow them to circulate in the bloodstream for an extended period [142]. For example, a study demonstrated the modification of MSNP carriers by applying a coating of RBC membrane and loading them with doxorubicin contributed to an extended circulation time. At pH 7.4, RBC membranes showed good stability, with negligible drug release (less than 5%) over 48 hours, and effectively inhibited the premature release of doxorubicin from the nanosystem resulting in efficient regulation of drug release. At pH 5.0, over 80% of drug release was achieved after 24 hours [143].

Macrophage membranes have been verified as suitable for coating MSNP carriers alongside RBC membranes. MSNP carriers coated with macrophage membranes can mimic nanosized macrophages due to the presence of macrophage surface proteins and their lipid bilayer structure [144]. In the work of Xuan *et al.* [145], the MSNP carriers were coated with macrophage membranes which led to a notable reduction in the phagocytic clearance of MSNP. After 24 hours of incubation, the macrophages completely engulfed pure MSNP, whereas more than 30% of the modified MSNP were seen circulating in the bloodstream. Furthermore, the silica (Si) element in the tumor was over 6% injected dose/g after the membrane coating, while MSNP without the membrane coating only reached 1.3% of the injected dose/g. These results demonstrate that macrophage cell membrane camouflaging of MSNP effectively reduces phagocytic clearance, and thus the efficacy of chemotherapy is highly enhanced [145]. In addition, cancer cells can evade the immune system by triggering processes that lead to weakened immune response, immunological suppression, and immune tolerance. CD47 is a transmembrane protein that is found on the surface of cancer cells. It plays a crucial role in immunological tolerance and preventing the engulfment of cancer cells by immune cells. The application of cancer cell membrane coating on MSNP can improve their compatibility with biological systems, extend their duration in circulation, reduce uptake by macrophages, and enable them to specifically target tumor cells through recognition of similar cell types. In Yue *et al.* [146] experiments, MSNP carriers were coated with the cell membranes of HepG2 cells and used to deliver berberine. The application of a cancer cell membrane coating resulted in increased accumulation of berberine in liver cancer tissue. Furthermore, a higher quantity of berberine was able to reach the cytoplasm of liver cancer cells compared to healthy cells. Additionally, this coating effectively prevented rapid blood clearance with only 5% of drug release at pH 7.4 and 55% of drug release at pH 5.5 after 96 hours [146].

Combination therapies and co-delivery

To date, multiple studies have focused on utilizing MSNP carriers as drug delivery vehicles for anticancer therapeutics such as 5-FU, carboplatin, capecitabine, cabazitaxel,

Table 2. MSNPs-based anticancer drug delivery.

Nanoparticle	Size (nm)	Entrapped drug(s)	Method used	Cancer type	Study Outcome	References
MSNP	199.3	5-FU	Template-assisted synthesis	Colon cancer	Enhanced internalization within colon cancer cells and higher accumulation in tumor tissues.	[155]
	300–320	Carboplatin	Surfactant-assisted approach	A549 and PC9 cells	Enhanced cytotoxicity and targeted drug delivery.	[9]
	140–600	Cabazitaxel	Surfactant-assisted approach	PC3 cells	Cytotoxic activity of cabazitaxel is improved with a higher free radical production when loaded onto MSNPs.	[69]
	245	Capecitabine	Modified Stober's method	HCT 116 cell lines.	Enhanced anti-tumor efficacy, higher drug uptake by HCT 116 cell lines with reduced toxicity.	[156]
	90	Camptothecin + doxorubicin (combo)	Sol-gel method	HeLa and U-87 MG cells	Targeted drug delivery and synergistic effect	[157]
	100–200	Cisplatin, carboplatin, oxaliplatin, and oxalipalladium	Template-assisted synthesis	A549, MCF7, HCT116, and HFF	Precise selectivity and targeted drug release, enhanced cytotoxicity, biocompatibility, solubility of entrapped drugs in comparison to individual free drugs.	[158]
	198–247	Curcumin and cisplatin	Sol-gel method	MES-SA/DX5	Excellent cytotoxic effects against resistance cancer cells.	[159]
	140	Dacarbazine	Modified Stober's method	B16F10 cells	High stability for drug retention, tumor acidic environmental responsiveness, and good biocompatibility.	[160]
	50	Docetaxel	One-pot and co-condensation of TEOS and APTS	MCF-7 cells	Enhanced cytotoxicity and increased apoptosis and necrosis with targeted accumulation of drug in tumor site.	[117]
	50–70	Docetaxel + 5-aza-2-deoxycytidine (combo)	Modified Stöber method	4T1 mammary tumor xenograft	The drug accumulated significantly at the tumor site with the use of dry cupping that resulted in a substantial reduction of tumor growth.	[161]
	90	Docetaxel + 8-hydroxyquinoline (combo)	Sol-gel method	MCF-7 cells	Enhanced cytotoxicity, little systemic toxicity, and targeted drug release (pH-dependent) at the tumor site.	[162]
	150	Doxorubicin + Paclitaxel combo	Biphase stratification	BT549 cells	Target specific and selective cytotoxic action against cancer cells (BT549) but had no inhibition effect on healthy normal breast cells (MCF-10A).	[163]
	76–90	Gemcitabine	Sol-gel method	MIA PaCa-2 cells	Targeted drug release and enhanced cytotoxicity of entrapped drug (even at lower conc = 10 μg/ml) compared to free drug.	[164]
	400–1000	Irinotecan	Modified Stöber synthesis	HT-29 cells	Enhanced cytotoxic effects compared to free drug.	[165]
	91.3–122.3	Irinotecan	Sol-gel method	MDA-MB-231 and 4T1 cell lines	Targeted drug delivery without drug leakage and off-target effects.	[166]
	56–73	Methotrexate	Sol-gel method	MCF7 breast cancer cells	Positive effect at a low dose (0.5 μM), Enhanced cytotoxicity compared to free drug formulation.	[71]
	350	Methotrexate	Surfactant templating method	MCF7 and A549 cell lines	Targeted drug release at the tumor site (pH 5.0, 7.4).	[167]

Nanoparticle	Size (nm)	Entrapped drug(s)	Method used	Cancer type	Study Outcome	References
	50	Paclitaxel	Sol-gel method	OVACAR-3 and PA-1 ovarian cancer cells	Targeted drug release, significantly reduced tumor progression.	[168]
	191–233	Paclitaxel	Sol-gel method	Pancreatic adenocarcinoma	Paclitaxel-loaded MSNPs showed reduced organ damage and leukopenia (*in vitro*).	[169]
	227.2	Paclitaxel + quercetin combo	Sol-gel method	MCF-7/ADR cells.	Extended tumor retention duration and potent anti-tumor efficacy without undesirable effects on healthy tissues (*in vivo*).	[170]
	190	Topotecan	Template-assisted synthesis	MDA-MB-231 xenograft model	High cellular uptake, apoptosis, and G0/G1 cell cycle arrest.	[171]

Abbreviations: 5-FU: 5-Fluorouracil; BT549: Breast cancer cell lines; BALB/c strain (4T1 cell line): Breast cancer cell line derived from the mammary gland tissue of a mouse; HeLa cells: Cervical cancer; U-87 MG cells: Glioblastoma; B16F10 cells: Murine melanoma cell line; MIA PaCa-2: Human pancreatic cancer cell lines; MES-SA/DX5: Human uterine sarcoma drug resistance cancer cell line; MDA-MB-231: Human breast cancer cell line; HT-29: Human colorectal adenocarcinoma cells; MCF-7: Human breast cancer cell line; HCT116: Human colorectal carcinoma cell line; HFF: Human foreskin fibroblasts cell line; A549: Human lung cancer cell lines; PC9: Lung adenocarcinoma cell line; MCF-7/ADR: Multidrug-resistant breast cancer cell line; OVACAR-3, PA-1: Ovarian cancer cells; and PC3: Prostate cancer cell lines.

cisplatin, curcumin, dacarbazine, docetaxel, doxorubicin, gemcitabine, irinotecan, oxaliplatin, oxalipalladium, paclitaxel, quercetin, and topotecan. Some interesting insights have been gained through these studies (Table 2). MSNP carriers have also shown promise in combination chemotherapy where multiple drugs such as camptothecin and survivin-shRNA with different mechanisms of action are administered simultaneously to enhance therapeutic efficacy. They can serve as adaptable nanocarrier systems for loading and delivering multiple drugs that allow for precise control over their release kinetics [147]. Combination chemotherapy can be accomplished by encapsulating multiple drugs into the pores of MSNP. Their distinctive characteristics, such as the large surface area and adjustable pore size, enable effective loading and precise release of chemotherapeutic drugs [148].

Combination therapy reduces adverse effects on healthy tissues while enhancing the cytotoxic effects of chemotherapy. For example, a unique core–shell-level MSNP nanosystem was developed by Sun *et al.* [149]. The core of the material included small mesopores filled with small-molecule drugs, while the shell had large mesopores linked to small interfering RNA (siRNA) through disulfide bonds. During therapy, the disulfide bonds in the shell of the treatment broke down by the tumor microenvironment. This phenomenon first released the siRNA, which inhibited the expression of P-glycoproteins and helped to reduce MDR. The small-molecule drug doxorubicin was then released from the core which led to a therapeutic effect. In an *in vivo* study, the tumor inhibition rate was 50.7% in mice treated with free doxorubicin, whereas it reached 87% in the group treated with doxorubicin-siRNA loaded on the hierarchical MSNP. This indicated a considerable inhibitory effect on drug resistance. Simultaneously, mice in the free doxorubicin group experienced weight loss, whereas mice in the other groups, including the doxorubicin-siRNA loaded on the hierarchical MSNP group, exhibited typical weight fluctuations. The therapeutic efficacy significantly improved in the administered anticancer treatment, and the side effects were greatly reduced compared to free drugs [149].

Moreover, a powerful anti-tumor "trident," which is a combination of radio-, immuno-, and anti-angiogenesis therapy based on mesoporous silica single-coated gold NPs, has shown synergistic effects. The nanosystem produced energy depositions when radiation was introduced and released the loaded toripalimab and bevacizumab, exhibiting significant anti-tumor properties [150]. The co-delivery of paclitaxel and gemcitabine was delivered with a nanocarrier using MSNP that aimed to achieve a synergistic effect in the treatment of pancreatic cancer by Meng *et al.* [151]. This combination showed excellent results compared to the delivery of free gemcitabine and abraxane in xenotransplantation and orthotopic tumor animal models. The therapeutic impact achieved was similar to a dose of abraxane that was 12 times higher [151]. Similarly, multifunctional MSNP carriers, including paclitaxel and a multidrug resistance reversal agent (tetrandrine), were researched by Jia *et al.* [152]. The findings on MCF-7 and MDR breast cancer cells (MCF-7/ADR) demonstrated that the MSNP formulation effectively suppressed the growth of drug-resistant cells and completely reversed their resistance to paclitaxel. Moreover, the nanoparticle loading drugs with a paclitaxel/ tetrandrine/ CTAB molar ratio of 4.4:1 completely reversed the resistance of MCF-7/ADR cells to paclitaxel with a resistance reversion index of 72.3. Mechanistic research showed that both tetrandrine and CTAB could arrest cells at the G1 phase, while paclitaxel arrested at the G2 phase.

Furthermore, MSNP can simultaneously deliver multiple therapeutic agents to obtain combination therapy. For instance, Li *et al.* [153] developed unique MSNP nanoplatforms that incorporated folic acid, photosensitizer, and silicon nanoparticles. The developed MSNP systems were synthesized by incorporating folic acid and modifying the photosensitizer 5,10,15,20-tetrakis (1-methyl 4-pyridinio) porphyrin tetra (p-toluenesulfonate) (TMPyP), which was first embedded within the MSNP. Subsequently, this MSNP was employed

for precise two-photon-excited fluorescence imaging-guided photodynamic treatment (PDT) and chemotherapy. During PDT, upon light exposure, the introduced TMPyP compound had the potential to generate singlet oxygen. In addition, the nanocomposite successfully prevented the disruption caused by natural fluorescence in biological systems by obtaining precise two-photon fluorescence cellular imaging using NIR laser excitation. Similarly, *in vitro* cytotoxicity testing revealed that a combination of PDT with chemotherapy (doxorubicin), which was referred to as synergistic therapy, exhibited a significant degree of therapeutic effectiveness against cancer cells [153].

Another study suggested sorafenib, which is a tyrosine kinase inhibitor, as a possible candidate for combination chemotherapy and photothermal therapy based on an MSNP platform for the treatment of hepatocellular carcinoma and tumor apoptosis. Gold (Au) nanoshells were used to create sorafenib-loaded Au-MSNP for photothermal conversion. Au-MSNP had a diameter of 104.3 nm with drug loading and entrapment efficiency of 22.4% and 51.3%. The study revealed an increase in sorafenib accumulation in hepatic tumor cells and provided better cancer suppression activity when loaded into an Au-MSNP nanosystem. The synergistic chemotherapy with photothermal action could improve the cytotoxicity of sorafenib and the rate of absorption in response to NIR radiation with 808 nm at a power density of 1 watt/cm^2 [154].

BIODISTRIBUTION AND SAFETY CONSIDERATIONS

General considerations

In general, silica-based materials are regarded as biocompatible and appropriate for the internal use of a living system (*in vivo*). Although MSNP carriers have undergone extensive research, however, no MSNP formulation has received FDA approval for medical use [172]. The composition of MSNP carriers consists of a SiO_2 matrix, which is vulnerable to nucleophilic attack by hydroxyl groups (–OH) from water in an aqueous environment. Consequently, the body produces orthosilicic acid, which is a biocompatible byproduct and is eliminated through the urine. While silica breakdown is challenging in physiological settings, the Si-O-Si combination remains stable. As a result of this particular behavior, the body builds up silica, which could pose a biosafety concern. Hence, it is imperative to enhance the biodegradation profile of silica-based nanocarriers for their use in clinical settings [173]. MSNP carriers, which have the same composition as typical silica nanoparticles, possess distinct characteristics that can potentially modify biological activities. Thus, the safety of cancer treatments using MSNP carriers through *in vivo* protocols should be investigated to assess their absorption, distribution, metabolism, excretion, and toxicity [174].

Previously, three different types of MSNP modifications were produced by Barguilla *et al.* [175]: bare MSNP, PEGylated MSNP (MSNP-PEG), and galacto-oligosaccharide-functionalized-MSNP (MSN-GAL). The genotoxicity and transforming ability of these MSNP delivery systems on human lung epithelial BEAS-2B cells were performed in both short term (48 hours) and long term (8 weeks). The initial 48-hour short-term treatments resulted in a dose-dependent rise in genotoxicity for cells treated with

MSNP-PEG, but not in oxidative DNA damage for cells treated with bare MSNP or MSN-GAL. Furthermore, no evidence of induced genotoxicity or oxidative DNA damage was identified even after 8 weeks of continuous exposure. However, the results of extended treatment with MSNP-PEG and MSNP-GAL showed the development of cell transformation characteristics. The increased ability of the cells to grow without anchorage, migrate, and invade were observed. In addition, the secretome derived from the cells treated with bare MSNP and MSNP-GAL exhibited specific tumor-promoting properties that enhanced both the quantity and size of HeLa cell colonies generated in an indirect soft-agar experiment. The results indicated that MSNP, particularly the functionalized ones, induced some detectable negative effects associated with the development of tumors [175].

Dosage, particle morphology, toxicity, and excretion pathways

In the case of pharmaceuticals, the saying "the dose makes the poison" indicates that the toxicity of drugs, including MSNP carriers, depends on the dosage. It is crucial to determine the concentration of MSNP that shifts from being therapeutic to becoming harmful. Furthermore, it is necessary to determine the type of toxicity from MSNP following both single (acute toxicity) and repeated (chronic toxicity) dosing. Additionally, it is necessary to compare several pathways of exposure [174]. When administered orally, MSNP carriers with an average diameter of 110 nm are absorbed into the bloodstream via the digestive system and subsequently accumulate in the liver. Over 7 days, their concentration initially rises after administration and eventually falls [176]. Although MSNP of comparable size can be given intravenously, they tend to accumulate mostly in the liver and spleen [132]. According to a study, MSNP carriers are biocompatible and undergo slow degradation into the non-toxic compound silicic acid $(Si(OH)_4)$ [177]. The distribution of MSNP carriers in the body is affected by the method of delivery, targeting ligands, and particle size [80,178]. Specifically, a study of quercetin-loaded MSNP carriers functionalized with folic acid primarily accumulated in breast tumors as an example [119]. Nevertheless, the immune and excretory systems rapidly eliminate MSNP after injection, which restricts their potential as nanocarriers [172]. Irrespective of the manner of delivery, most MSNP carriers are excreted through urine and feces [179].

Studies on animal models

MSNP morphology and distribution

There is limited research available on the impact of the morphology of MSNP carriers on their behavior in experimental animals. Huang *et al.* [180] developed multiple MSNP carriers with comparable particle size, chemical makeup, and surface charge but varied in their aspect ratios between length and width. These nanoparticles were taken up by tumor cells via non-specific cellular uptake. Additionally, *in vitro* experiments revealed that particles with a higher aspect ratio (elongated rod form) were absorbed in higher amounts and exhibited a faster rate of internalization compared to particles with an aspect ratio of 1 (spherical shape). Thus, variations in

the curvature of MSNP may account for this distinct behavior. Furthermore, rod-shaped MSNP carriers would possess a greater contact area with the cell membrane compared to spherical MSNP carriers due to the interaction between the longitudinal axis of the rod and the cell membrane. The influence of the shape of MSNP carriers on their biodistribution, clearance, and biocompatibility was also examined by employing MSNP with various aspect ratios. Short-rod MSNP carriers were mostly found to accumulate in the liver, while long-rod MSNP carriers had a higher tendency to get trapped in the spleen. Following the process of PEGylation, there was an observed rise in the concentration of MSNP carriers in the lung. The influence of the form of MSNP carriers on biocompatibility, namely in terms of hematological, serum chemistry, and histopathology, was not evident [180].

In an *in vivo* study, MSNP carriers (size 80–360 nm) predominantly accumulated in the liver and spleen in albino BALB/c mice with 4T1 mammary carcinoma. Smaller amounts of these nanoparticles were found in the lungs, kidneys, and heart. However, when injected into nude mice with subcutaneous tumors, MSNP carriers measuring 100–130 nm underwent absorption in the spleen and liver [181]. Recent research by Choudante *et al.* [63] explored a new method to overcome the abnormal alterations caused by MSNP administration in the delivery of anticancer drugs. The study also investigated the biocompatibility of MSNP systems. Tin-conjugated MSNP called S3 was reported to have an increased ability to selectively kill breast cancer cells in a laboratory setting. The suppression of breast tumor growth in mice was performed *in vivo* anticancer experiments using S3 in a BALB/c mice model. The findings revealed an elevated proportion of reactive oxygen species generation, a greater number of apoptotic cells, and a drop in the

expression of the Ki-67 protein, which suggested a decline in cell growth and anti-tumor effects. The safety evaluation of S3 as an anticancer agent found no notable abnormalities in various organs or alterations in serum biochemical parameters of tumor mice, which indicated that S3 did not impact fundamental metabolism. Further genotoxicity experiments verified that S3 did not demonstrate clastogenic, aneugenic, or mitotoxic characteristics in the bone marrow cells of Swiss albino mice. In addition, S3 exhibited excellent biocompatibility and did not cause any histopathological alterations in the vital organs of mice [63]. Supportively, doxorubicin-loaded MSNP carriers had an average size of 200 nm and provided a specific target at tumor cells. This formulation exhibited minimal accumulation in the kidneys and liver (Fig. 7) [182].

Impact of shear stress and shape on toxicity

Recently, the influence of form and shear stress on the toxicity of MSNP carriers after injection was evaluated by Niroumand *et al.* [88]. A laboratory-based blood flow model was created to examine the harmful effects and the underlying mechanisms of spherical MSNP and rodlike MSNP particles on HUVECs. The findings indicated that the interactions between MSNP and HUVECs under the physiological flow conditions differed significantly from those under static settings. Regardless of whether the settings were either static or under flow conditions, the rod-shaped MSNP particles exhibited superior cellular uptake and lower oxidative damage compared to spherical MSNP particles. The primary cytotoxicity mechanism caused by rod-shaped MSNP was the result of shear stress-dependent mechanical harm to the cell membrane. However, the toxicity of spherical MSNP was linked to both mechanical harm and oxidative damage. By including fetal bovine serum,
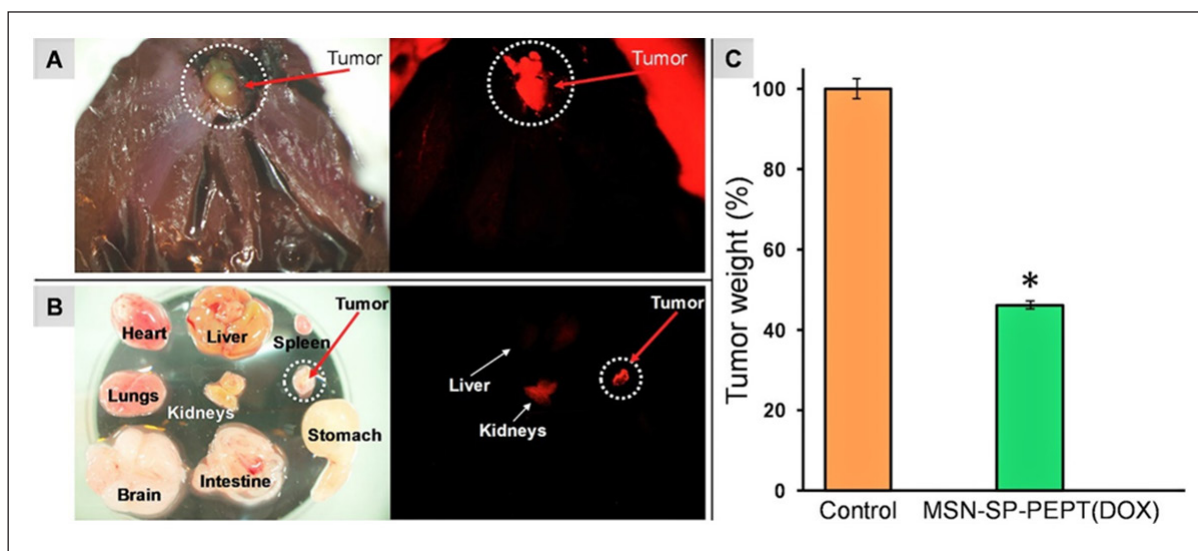

Figure 7. (A) Fluorescence microscopy showing the biodistribution of MSNP-SP-PEPT 48 hours after injection. Left: (bright field); right: (red fluorescence). Red fluorescence from the labelled nanoparticles was seen in the tumor, confirming their passive accumulation by the enhanced permeability and retention effect. (B) The organs and tumors from the dissected chicken embryo are visible. MSNP-SP-PEPT specifically targeted the tumor and exhibited minimal liver and kidney accumulation. (C) 100 μg/ml of DOX-loaded MSNP-SP-PEPT inhibited the formation of tumors. In this preliminary study, the nanocarrier showed the ability to decrease the tumor weight by 50% after 72 hours (*$p < 0.05$ *vs.* control). Reprinted with permission from [182].

the adverse effects of spherical MSNP were mitigated by the reduction of cellular absorption and oxidative stress, both in static and flow settings. Furthermore, the *in vivo* findings demonstrated that both spherical MSNP and rod-shaped MSNP particles induced cardiovascular damage in zebrafish and mouse models as a result of elevated shear stress, particularly in the heart. Spherical MSNP-induced substantial oxidative damage in mice at the accumulation site that included the liver, spleen, and lung. On the other hand, rod-shaped MSNP did not result in significant oxidative stress. Hence, the shape of particles and the force of blood flow are essential factors in determining the safety of MSNP-based therapy [88].

Maximum tolerated dose and subacute toxicity

Lu *et al.* [183] investigated the highest intravenous dose of fluorescent MSNP carriers that could be tolerated by female nude mice. The dosage that varied from 10 to 200 mg/kg was administered once daily for 10 days. The findings demonstrated that the overall health of all mice was satisfactory. However, mice with doses over 100 mg/kg had certain changes in liver enzymes. Long-term toxicity assessments conducted on healthy nude mice with a daily dosage of 1 mg per animal revealed no abnormal reactions over 2 months [183]. Recently, the primary structures of MSNP carriers and their subacute toxicity were examined in mice. Following two weeks of MSNP (dose 50, 100, and 200 mg/kg/d) carrier administration directly into the stomach as an intragastric route, notable increases were observed in the blood levels of alkaline phosphatase, alanine transaminase, aspartate aminotransferase, and tumor necrosis factor-alpha. Additionally, infiltration of inflammatory cells in the spleen and intestines was also observed. MSNP carrier administration resulted in oxidative stress in the intestine and the death of colonic epithelial cells in mice. Intestinal epithelial cells displayed mitochondrial ridge breakage and a decrease in membrane potential following treatment with MSNP carriers. In addition, MSNP elevated the levels of reactive oxygen species while suppressing the expression of autophagy proteins. MSNP carriers had a considerable impact on the diversity of intestinal flora in mice, particularly on harmful microbes that resulted in an imbalance in intestinal microecology. Meanwhile, MSNP showed an impact on the production of metabolites that played a role in several metabolic pathways, such as pyrimidine metabolism, central carbon metabolism in cancer, protein digestion and absorption, mineral absorption, ABC transport, and purine metabolism. The subacute toxicity of MSNP primarily arises from intestinal injury [184].

Long-term toxicity and pathology

Mohammadpour *et al.* [184] investigated the toxicity of non-surface modified MSNP in female and male BALB/c mice for 1 year. The effects of different sizes and porosities of the silica nanoparticles (46 and 432 nm) and MSNP (466 nm) when administered intravenously as a single dose to female and male BALB/c mice (10 animals/sex/group) were investigated. Based on the clinical observations and analysis of blood parameters, the results showed no notable alterations in body weight, cell blood count, or plasma biomarker indices. The post-necropsy assessment of internal organs and organ-to-body weight ratio did not show any significant changes.

Nevertheless, a thorough microscopic analysis unveiled a notable presence of liver inflammation and clusters of histocytes accompanied by neutrophils in the spleen, which indicated the presence of an ongoing or healing injury. The rapid buildup of these nanoparticles in the liver and spleen following intravenous delivery, along with the time required for their elimination, resulted in the injury. Furthermore, there were slight alterations attributable to prior heart attacks or resolved blood clots within blood arteries. These alterations consisted of calcifications in the pulmonary vessels, localized scarring of the heart with calcifications, and localized damage to the kidneys. The majority of the pathological abnormalities were identified with the administration of large, impermeable MSNP. No statistically significant chronic toxicity was detected for either the small non-porous particles or the MSNP. After 1 year, post-exposure assessment showed that both female and male BALB/c mice required a minimum of 12 months to fully recover from the acute tissue toxic effects caused by MSNP when administered intravenously at their maximum tolerated dose over a single treatment period of 10 days. In addition, *in vitro* experiments using human blood and plasma demonstrated that the nanoparticles did not cause hemolysis or activate the complement system after incubation [185].

Hepatotoxicity and oxidative stress in liver

MSNPs with a size of 109 nm were tested for hepatotoxicity by Zhang *et al.* [185]. The findings showed that the particles reduced the cell viability of human hepatic L02 cells in a concentration-dependent manner; at a concentration of 120 µg/ml, the cell viability dropped by around 33% compared to 5 µg/ml. Additionally, the *in vivo* results showed that MSNPs were toxic in a dose-dependent manner. In BALB/c mice, intravenous administration of MSNP at a dose of 50 mg/kg increased the serum concentration of alanine aminotransferase (ALT) and aspartate aminotransferase (AST), which are markers of liver function, by approximately 74% and 61%, respectively, in comparison to intravenous administration of MSNP at a dose of 12.5 mg/kg [186].

Another study investigated the mechanisms of MSNP liver damage in a rat model. For 30 days, MSNPs at doses of 25, 50, 100, and 200 mg/kg were administered to the test group. The findings showed that the concentration of ALT and AST in the blood increased in a concentration-dependent manner. The group receiving MSNP at the 200 mg/kg dose had higher levels of ALT and AST than those receiving 25 mg/kg, increasing by 39 and about 15%, respectively. The histopathology results supported these findings, showing that the animals receiving 200 mg/kg of MSNP had more severe pathological lesions than the group receiving 25 mg/kg. Additionally, the findings of assessments of ROS, MDA, and NO showed that these parameters rose in correlation with the MSNP concentration, suggesting that MSNP enhanced the production of ROS and oxidative stress in liver tissues. However, the concentration of GSH, SOD, and CAT was inversely correlated with the quantity of MSNP, suggesting that MSNP inhibited the liver's antioxidants, CAT, SOD, and GSH. The outcomes further showed that MSNP inhibited the PPARγ signaling pathway in

hepatocytes, which is essential for the suppression of fibrosis, and inflammation, and controlling the expression of antioxidant enzymes [187].

Toxicity reduction through functionalization

Functionalized MSNP as a drug delivery vehicle remains primarily in the bloodstream and results in a significantly reduced risk of kidney and liver injury. MSNP of larger particle sizes is retained on the surface of the epidermis layer with a reduced ability to penetrate the skin. At the same time, smaller MSNP can easily penetrate through the layers of the skin. MSNPs with long rod shapes seem to accumulate mostly in the spleen, whereas MSNPs with short rod shapes exhibit greater deposition in the liver. Finally, it is essential to conduct additional assessments of the cytotoxicity and biocompatibility of MSNP carriers before they are employed in biological contexts, such as cancer treatment [188]. Thus, the relationships between MSNP and living systems, such as cells, tissues, and organs, are an important component of evaluating biocompatibility. This evaluation aims to determine whether MSNP can cause organ damage, inflammation, or adverse effects. Animal models can be used in live experiments to clarify the biocompatibility of MSNP [66].

Another crucial factor to consider is the optimization of the size and surface charge of MSNP. It has been observed that smaller MSNP particles at 20 nm tend to exhibit greater biocompatibility and cellular uptake. Likewise, the surface charge can be modified to minimize nonspecific interactions and adverse effects [189]. Various approaches can be employed to enhance the biocompatibility of MSNP systems and mitigate potential toxicity. Initially, the MSNP surface can be altered by incorporating biocompatible polymers such as chitosan and PEG that enhance stability, minimize unintended interactions with biological components, and decrease immune responses to encapsulated drugs, such as 5-FU [190] and doxorubicin (Fig. 8) [191].
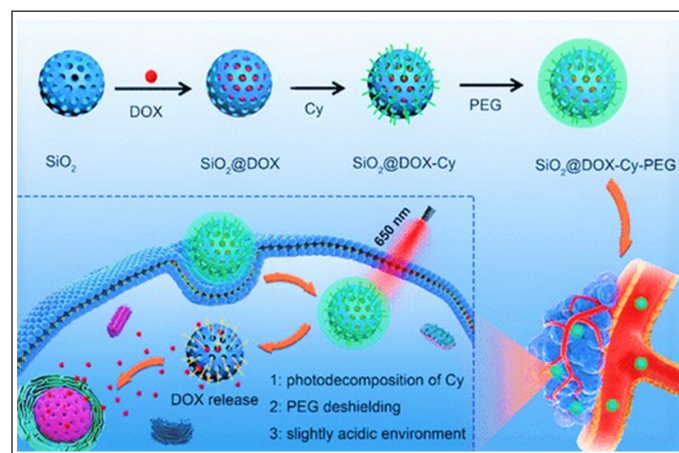

Figure 8. Photosensitive triggered polyethylene glycol-coated MSNP with entrapped doxorubicin (SiO$_2$@DOX) reduces nonspecific interactions with biological components and possesses on-demand anticancer drug delivery. Reprinted with permission from [191].

Nevertheless, research conducted on female CD-1 mice demonstrated that the maximum tolerated dose of MSNP was merely 30 mg/kg. The kidney and lungs were the primary organs impacted beyond the maximum tolerable dose. By introducing amine groups, the toxicity of MSNP carriers was reduced, which allowed for an increase in the maximum tolerated dose to 150 mg/kg [192]. The lethal dose (LD$_{50}$) of 110 nm rattle-type MSNP carriers with a hollow structure was found to be greater than 1,000 mg/kg when administered as a single dose. Furthermore, no deaths were detected when a repeated dose of 80 mg/kg was administered for 14 days. The coefficients of liver and spleen significantly elevated after injection at 500 and 1,280 mg/kg of MSNP compared with the control group ($p < 0.05$). The mice treated with MSNP at 1,280 mg/kg showed changes such as loss of appetite, weight loss, and passive behavior, and 6 mice died in 3 days. The liver was the primary target organ that was exposed to high doses and showed signs of necrosis, lymphocyte infiltration, and degradation. After injecting at 500 and 1,280 mg/kg, spleen samples revealed no significant changes in the size of the red pulp or the micro-morphology of the lymphoid follicles, although splenic coefficients increased significantly [193]. Safety assessment studies of mercaptopropyltriethoxysilane ligand functionalized MSNP in BALB/c mice revealed no significant abnormalities in major organs. Results showed no changes in serum biochemical parameters, suggesting that it did not affect basic metabolism. The nanosystem was non-genotoxic, without clastogenic, aneugenic, or mitotoxic properties in the bone marrow cells, and demonstrated high biocompatibility [63]. Doxorubicin-loaded MSNP functionalized with azide-modified β-cyclodextrin followed by GPLGVRGRGDK-Ad peptide and DOX-MSNP-CD-peptide-PEG with a size of approximately 300 nm specifically accumulated in the tumor. The peptide is degraded by the MMP-2 overexpressed enzyme in tumors, while the MSNP core could be degraded due to glutathione. Pharmacokinetic studies using 4T1 tumor-bearing BALB/c mice revealed an AUC of 442.4 h^{-1} for the developed nanosystem (compared to 133.0 h^{-1} for free drug), with half-life improved to around 0.89 hours. The nanosystem demonstrated high accumulation in tumor, followed by the liver, lungs, spleen, kidneys, and heart. However, the study lacks results mentioning biochemical parameters for assessing potential tissue damage or effects in these organs [38].

EMERGING ADVANCEMENTS

The field of drug delivery systems based on MSNP is undergoing rapid advancement. Various emerging technologies, such as optimizing drug loading, employing surface functionalization strategies, utilizing combination approaches, and achieving synergistic drug delivery with other nanoparticles such as hydrogels, gold NPs, and carbon nanotubes, are expected to play a significant role in shaping the development of MSNP drug delivery systems [80]. Current research efforts are focused on optimizing the procedures used to load drugs onto MSNP carriers and enhancing the features that allow for controlled release. This involves the development of stimuli-responsive MSNP that may release drugs in response to specific signals such as pH, temperature, or enzyme activity [194,195].

In another publication, liposome-fused MSNP carriers were created as a "protocell" structure that was able to transport through cell membranes. Unlike other delivery systems, a protocell is a unique carrier that has the characteristics of liposomes, such as minimal immunogenicity and toxicity. It can also be PEGylated to enhance its circulation duration and half-life or conjugated for targeted drug delivery. Protocells employ the mesoporous core features to effectively manage both loading and release. Finally, protocells exhibit greater stability compared to liposomes alone [196].

In the future, there is an expectation for combination therapies using MSNP systems to become more prevalent. This will enable the combination of multiple drugs, immunotherapies, or imaging agents within MSNP that will result in synergistic effects and individualized treatment approaches [197]. The targeting capabilities of MSNP will be improved through advancements in surface modification techniques and ligand design to allow for more precise delivery to certain cell types or regions [198,199]. Combining MSNP with other nanomaterials, such as metallic nanoparticles, dendrimers, quantum dots, and carbon nanotubes, holds the potential to further enhance drug delivery, imaging, therapeutic efficacy, and cancer immunotherapy enhancement [200,201].

The incorporation of certain ligands into MSNP carriers can influence the distribution of these nanosystems throughout the organs, which can consequently alter their safety profile. PEGylation of MSNP significantly enhances their compatibility with blood, which results in a much-reduced hemolysis effect. It also reduces the non-specific binding to serum proteins, which in turn increases the half-life of MSNP carriers. This is most likely due to MSNP carriers evading identification by the reticuloendothelial system [29]. Meng *et al.* [201] presented the distribution of MSNP carriers with various particle sizes (80, 120, 200, and 360 nm) and their corresponding PEGylated versions. As expected, the duration of blood circulation for PEG-MSNP comparatively increased. Regardless of their size, both MSNP and PEG-MSNP carriers primarily accumulated in the liver and spleen following intravenous injection into the tail. This is because the liver and spleen phagocytes recognized and engulfed the MSNP. However, small amounts of MSNP carriers were detected in the lungs and kidneys and at a smaller amount in the heart. Both MSNP and PEG-MSNP carriers with larger particle sizes were more readily trapped by the organs, hence promoting breakdown. PEG-MSNP carriers with smaller particle sizes were able to evade capture by the liver, spleen, and lung tissues more effectively. They also had a longer half-life in the bloodstream and were biodegraded at a slower rate, which resulted in reduced excretion rates [202].

Multiple *in vitro* studies have shown that MSNP carriers might cause cell death in various cell lines. However, it has been reported that the presence of residual structure-directing agents, particularly ionic surfactants can lead to significant cytotoxicity when MSNP carriers are produced by conventional extraction methods and surfactants are incompletely removed [203]. To achieve this goal, several issues need to be addressed, such as potential biodistribution, clearance mechanisms, and the ultimate fate of MSNP carriers in the body after administration. The performance of each drug compound or formulation is normally assessed based on the rate and degree of adsorption, distribution, metabolism, and elimination. MSNP carriers are commonly administered by intravenous or oral routes. However, absorption and the distribution of MSNP carriers exhibit significant variations that depend on the route of delivery [204].

CLINICAL TRIALS AND REGULATORY CHALLENGES

As of March 12, 2025, there have been no clinical trials specifically focused on MSNPs for anticancer drug delivery. However, various silica-based nanosystems have advanced through clinical trials, offering valuable insights into their clinical applications and safety profiles. MSNP are part of the broader family of silica-based nanosystems, characterized by a silica framework, yet they differ in porosity. Despite these similarities, there are notable differences between MSNP and other clinically studied silica-based nanosystems. Many of these systems, such as AmSil® (amorphous silica nanoparticles) and Cornell dots (C-dots, ultrasmall silica nanoparticles), are non-porous or have different pore structures, which may influence their biodistribution profiles. Clinically studied silica-based nanosystems have largely been explored for imaging, diagnostics, and passive drug delivery, rather than the active tumor-targeted therapies typical of MSNP [205]. One study investigated the bioavailability of fenofibrate loaded onto MSNP compared to the commercially available formulation Lipanthyl® in 12 healthy male volunteers. The results indicated good tolerance and enhanced bioavailability of fenofibrate (a fibric acid derivative used as an antilipidemic agent) [206]. Another study (ACTRN12618001929291) assessed the safety, tolerability, and pharmacokinetics of a silica-lipid hybrid formulation loaded with simvastatin in healthy males ($n = 12$). The findings showed a 3.5-fold improvement in bioavailability compared to the commercial formulation, with no side effects observed following oral administration [207]. A similar Phase 1 study evaluated the safety of ibuprofen-loaded silica-lipid hybrid nanoparticles through physical examinations, clinical tests (e.g., hemoglobin, red blood cell count, platelets, white blood cell count, urinalysis), and reports of adverse events in healthy males ($n = 16$). The study confirmed that there were negligible acute side effects associated with the formulation [208].

Silica-based nanosystems first gained attention in clinical therapy research in 2007 for treating atherosclerotic lesions via plasmonic photothermal therapy (NCT01270139). Long-term results, reported in 2017, showed that patients treated with silica-gold nanoparticles experienced no cytotoxicity or clinical issues, demonstrating superior safety, lower mortality rates, and reduced target lesion revascularization compared to stent-based treatments. The only reported case of toxicity occurred in 2010, during the development of CD68-targeted microbubbles using silica-gold iron nanoparticles to target macrophages in atherosclerotic plaques (NCT01436123). The trial was terminated after patients receiving the nanoparticle treatment showed signs of toxicity, leading to the discontinuation of the microbubble-based therapy. A distinct approach involving C-dots was approved by the FDA in 2012

Table 3. Clinical trials involving silica-based nanosystems (ClinicalTrials.gov, retrieved on March 12, 2025).

Clinical trial number	Type	Phase	Masking	Purpose	Clinical use	Start date	Participants	Status
NCT01436123	CD68-targeted microbubbles silica-gold-iron NPs	Phase 1	Double (Participant and Investigator)	Treatment	Atherosclerosis	December 2010	62	Terminated (October 2012)
NCT01270139	Silica-gold-Iron bearing NPs	NA	Double (Participant and Investigator)	Treatment	Atherosclerosis	April 2007	180	Completed (August 2016)
NCT02680535	PEGylated silica nanoshell	NA	None (Open Label)	Treatment	Neoplasms of the Prostate	February 2016	45	Completed (October 2020)
NCT04240639	PEGylated AuroShell particle infusion	NA	None (Open Label)	Treatment	Neoplasms of the Prostate	January 2020	60	Active, not recruiting. Estimated completion date (June 2023)
NCT04656678	PEGylated silica nanoshell	NA	None (Open Label)	Treatment	Prostate cancer	November 2020	200	Recruiting (Last update posted February 2024) Estimated completion date (October, 2025)
NCT01266096	cRGDY-PEG-C-dots	NA	None (Open label)	Diagnostic	Brain tumor	January 2011	23 (5 newly diagnosed or recurrent melanoma and 18 malignant brain tumor patients)	Active, not recruiting. Estimated completion date (December 2025)
NCT02106598	Fluorescent cRGDY-PEG-Cy5.5-C dots	Phase 1 and Phase 2	None (Open Label)	Diagnostic	Head and neck melanoma	April 2014	67	Active, not recruiting. Estimated completion date (April 2025)
NCT03465618	89Zr-DFO-cRGDY-PEG-Cy5-C' dot particles	Phase 1	Single (Outcomes Assessor)	Diagnostic	Brain cancer, and pituitary adenoma	March 2018	17	Active, not recruiting. Estimated completion date (March 2025)
NCT04167969	64Cu-NOTA-PSMAi-PEG-Cy5.5-C' dots	Phase 1	None (Open Label)	Diagnostic	Prostate cancer	February 2021	10	Recruiting. Estimated completion date (November 2026)

for their use in the initial phase of clinical trials. C-dots are ultrasmall inorganic silica nanoparticles (6–10 nm in diameter) developed for fluorescence imaging, specifically for detecting sentinel lymph nodes prior to cancer surgery. To date, C-dots have been applied in patients with metastatic melanoma, malignant brain tumors, and head and neck melanoma (NCT01266096, NCT02106598, NCT03465618). As of March 12, 2025, no adverse effects or hazards have been reported in relation to these nanoparticles, suggesting they are safe for use in human cancer diagnostics. Due to their small size, C-dots are rapidly cleared by the kidneys, alleviating concerns over silica nanoparticle bioaccumulation. The latest clinical trials based on this technology include the use of 64Cu-NOTA-PSMA-PEG-Cy5.5-C dots to identify tumor cells before and during prostate cancer surgery (NCT04167969). Additionally, various studies involving PEGylated gold-silica nanoshells are being conducted by AuroLase (Nanospectra Biosciences) for the treatment of prostate, and head and neck cancer (NCT00848042, NCT02680535, NCT04240639, and NCT04656678). After intravenous injection, these AuroShell particles preferentially accumulate in tumors via the EPR effect, followed by thermal ablation of the tumor using NIR stimulation. Updates on clinical trials involving silica-based nanosystems can be found in Table 3, sourced from ClinicalTrials.gov as of March 12, 2025.

Although the number of silica-based nanosystems translated into human clinical trials remains limited, the trials conducted on solid silica nanoparticles so far indicate that silica is safe for human use and can enhance therapeutic efficacy. In the context of this review, these clinical trials provide indirect support for the potential of MSNPs in clinical applications, albeit with a narrow focus, primarily validating the biocompatibility and systemic behavior of silica-based nanocarriers rather than the therapeutic efficacy of MSNP-based drug delivery systems. Consequently, additional clinical trials are crucial to bridge the gap between preclinical research and clinical application. Table 4 shows the comparison of key features of MSNPs with clinically approved nanocarriers such as liposomal doxorubicin (Doxil™, Caelyx™, Myocet™), Abraxane™ (albumin-bound paclitaxel), and PEGylated nanoparticles, including aspects such as circulation half-life, excretion routes, regulatory approval, and the progress of clinical trials.

In this review article, we discussed that while MSNPs have demonstrated biocompatibility in preclinical models, their long-term toxicity, biodegradation, and clearance mechanisms

Table 4. Comparison of MSNP with clinically approved nanocarriers.

Feature	MSNP	Liposomal Doxorubicin	Abraxane™ (Albumin-bound Paclitaxel)	PEGylated Nanoparticles	References
Drug encapsulation	Adsorption within mesopores	Lipid bilayer	Non-covalent binding to albumin	Surface adsorption or entrapment	[209,210]
Controlled drug release	pH-sensitive, enzyme-responsive, redox-sensitive	Slow release via liposomal breakdown	Passive release by albumin degradation	Slow release based on PEG density	[209]
Circulation half-life	Shorter, but extended with RBC membrane coating (18.2 hours)	20–30 hours	27 hours	More than 4 hours	[143,209,211]
Excretion route	Renal or hepatobiliary (size-dependent)	Hepatobiliary	Fecal excretion (20% of the total dose administered), while less than 1% of the total administered dose was excreted in urine as the metabolites 6α-hydroxypaclitaxel and 3'-p-hydroxypaclitaxel.	Hepatobiliary	[209,212]
Regulatory approval	No clinical approval yet	Doxil™, Caelyx™ (PEGylated), and Myocet™ (non-PEGylated). Doxil™ (Bridgewater, NJ, USA) FDA-approved in 1995. Caelyx™ (Kenilworth, NJ, USA) approved by the European Medicines Agency (EMA) in 1996. Myocet™ (Castleford, UK) approved by the EMA in 2000.	FDA-approved (2005)	PEGylated nanoparticles FDA-approved.	[209,213]
Clinical trials	No MSNP-based anticancer drug in trials	Many completed for various cancers	FDA-approved for breast, lung, and pancreatic cancer	Several PEGylated formulations FDA-approved	[209]

Note: Key information (circulation half-life, excretion route) given in the table for the marketed product Abraxane® was retrieved from patent information chart with specifications as follows (Product No. 103450, NDC No. 68817-134-50, and U.S. Patent Numbers: 5,439,686; 5,498,421; 6,096,331; 6,506,405; 6,537,579; 6,749,868; 6,753`,006) filed by the company ABRAXIS ONCOLOGY, A Division of Abraxis BioScience, Inc. Los Angeles, CA 90049, Issued on May 2007

in humans remain unclear. Regulatory agencies such as FDA and EMA require detailed toxicokinetic studies to assess their accumulation, metabolism, and potential toxicity in vital organs. Literature suggests that MSNPs can trigger pro-inflammatory responses and induce immune system activation, which should be thoroughly evaluated in *in vivo* immunotoxicity studies [184]. As discussed in section 5, many preclinical MSNP studies are performed in murine models [181,63,182,183], which may not fully predict human responses. Clinical translation of MSNPs requires further validation in non-human primates and canine models that are more relevant to human pharmacokinetics and efficacy. Since MSNPs represent a novel drug delivery system, first-in-human clinical trials will require extensive Investigational New Drug applications with comprehensive safety and pharmacokinetic data.

CONCLUSION

In conclusion, after thoroughly summarizing the literature, MSNP doses above 100 mg/kg induce elevated ALP, ALT, AST, and TNF-alpha levels in the blood, indicating liver stress. A daily dose of 1 mg over 2 months is safe in female nude mice, but sub-acute doses (100–200 mg/kg/day) lead to liver and intestinal oxidative stress. Intravenous administration of MSNP sizes from 46 to 466 nm triggers liver and spleen inflammation, with larger particles (above 400 nm) causing acute tissue damage that took 12 months to recover. In female CD-1 mice, a maximum tolerated dose of 30 mg/kg was observed, while amine modification raised tolerance to 150 mg/kg. Rattle-type MSNPs (110 nm) have an LD_{50} above 1,000 mg/kg, showing no toxicity at repeated 80 mg/kg intravenous doses over 14 days. In human hepatic L02 cells, MSNP at 120 µg/ml reduced cell viability by 33%, and intravenous MSNP at 50 mg/kg significantly elevated ALT and AST. In rats, doses of 25–200 mg/kg over 30 days caused dose-dependent liver toxicity, oxidative stress, and reduced antioxidant enzyme levels, suggesting higher doses suppress natural liver defenses. Given the toxicological profile details of MSNP, questions remain regarding the toxicological and biodistribution assessments to properly evaluate and ensure the long-term safety of MSNP platforms. Three Phase 1 clinical studies conducted in healthy individuals indicate no signs of chronic adverse events using MSNP formulations, as confirmed by physical examinations and clinical tests. Despite current research attempts, we suggest long-term toxicological evaluation studies to fully comprehend both the usefulness and awareness of MSNP carriers. Lastly, we are hopeful that functionalized MSNP systems which have already shown promising findings in preclinical studies, will represent an exciting breakthrough in nanomedicine, enhancing cancer therapy outcomes in the near future.

ACKNOWLEDGMENT

AUTHOR CONTRIBUTIONS

All authors made substantial contributions to conception and design, acquisition of data, or analysis and interpretation of data; took part in drafting the article or revising it critically for important intellectual content; agreed to submit to the current journal; gave final approval of the version to be published; and agree to be accountable for all aspects of the work. All the authors are eligible to be an author as per the International Committee of Medical Journal Editors (ICMJE) requirements/guidelines.

FINANCIAL SUPPORT

CONFLICTS OF INTEREST

The authors report no financial or any other conflicts of interest in this work.

ETHICAL APPROVALS

This study does not involve experiments on animals or human subjects.

DATA AVAILABILITY

All the data is available with the authors and shall be provided upon request.

PUBLISHER'S NOTE

All claims expressed in this article are solely those of the authors and do not necessarily represent those of the publisher, the editors and the reviewers. This journal remains neutral with regard to jurisdictional claims in published institutional affiliation.

USE OF ARTIFICIAL INTELLIGENCE (AI)-ASSISTED TECHNOLOGY

The authors declare that they have not used artificial intelligence (AI)-tools for writing and editing of the manuscript, and no images were manipulated using AI.

REFERENCES

1. Batool S, Sohail S, ud Din F, Alamri AH, Alqahtani AS, Alshahrani MA, *et al.* A detailed insight of the tumor targeting using nanocarrier drug delivery system. Drug Deliv. 2023;30:2183815.

2. Ulldemolins A, Seras-Franzoso J, Andrade F, Rafael D, Abasolo I, Gener P, *et al.* Perspectives of nano-carrier drug delivery systems to overcome cancer drug resistance in the clinics. Cancer Drug Resist. 2021;4:44.

3. Parveen N, Sheikh A, Abourehab MA, Karwasra R, Singh S, Kesharwani P. Self-nanoemulsifying drug delivery system for pancreatic cancer. Euro Poly J. 2023;190:111993.

4. Woodring RN, Gurysh EG, Bachelder EM, Ainslie KM. Drug delivery systems for localized cancer combination therapy. ACS Appl Bio Mat. 2023;6:934–950.

5. Wang C, Xiao J, Hu X, Liu Q, Zheng Y, Kang Z, *et al.* Liquid core nanoparticle with high deformability enables efficient penetration across biological barriers. Adv Healthcare Mat. 2023;12:2201889.

6. Dhar R, Gorai S, Devi A, Jha SK, Rahman MA, Alexiou A, *et al.* Exosome: a megastar of future cancer personalized and precision medicine. Clin Transl Discovery 2023;3:e208.

7. Ezike TC, Okpala US, Onoja UL, Nwike PC, Ezeako EC, Okpara JO, *et al.* Advances in drug delivery systems, challenges and future directions. Heliyon. 2023;9:e17488.

8. Moholkar DN, Kandimalla R, Gupta RC, Aqil F. Advances in lipid-based carriers for cancer therapeutics: liposomes, exosomes and hybrid exosomes. Cancer Lett. 2023;565:216220.

9.   Radhakrishnan D, Patel V, Mohanan S, Ramadass K, Karakoti A, Vinu A. Folic acid functionalised mesoporous core-shell silica nanoparticles loaded with carboplatin for lung cancer therapy. Microporous Mesoporous Mater 2023;360:112708.

10. Dumontel B, Conejo-Rodríguez V, Vallet-Regí M, Manzano M. Natural biopolymers as smart coating materials of Mesoporous Silica nanoparticles for drug delivery. Pharmaceutics. 2023;15:447.

11. Kolimi P, Narala S, Youssef AAA, Nyavanandi D, Dudhipala N. A systemic review on development of mesoporous nanoparticles as a vehicle for transdermal drug delivery. Nanotheranostics. 2023;7:70.

12. Sutrisno L, Ariga K. Pore-engineered nanoarchitectonics for cancer therapy. NPG Asia Mater. 2023;15:21.

13. Sarkar S, Ekbal Kabir M, Kalita J, Manna P. Mesoporous Silica nanoparticles: drug delivery vehicles for antidiabetic molecules. ChemBioChem. 2023;24(7):e202200672.

14. Almomen A, Alhowyan A. A comprehensive study on folate-targeted mesoporous silica nanoparticles loaded with 5-fluorouracil for the enhanced treatment ofgynecological cancers. J Funct Biomat. 2024;15:74.

15. Tripathi AD, Labh Y, Katiyar S, Singh AK, Chaturvedi VK, Mishra A. Folate-mediated targeting and controlled release: PLGA-encapsulated mesoporous silica nanoparticles delivering capecitabine to pancreatic tumor. ACS Appl Bio Mater. 2024;7(12):7838–51.

16. Li Y, Phan VG, Pan Z, Xuan X, Yang HY, Luu CH, *et al.* Integrated and hyaluronic acid-coated mesoporous silica nanoparticles conjugated with cisplatin and chlorin e6 for combined chemo and photodynamic cancer therapy. Euro Poly J. 2024;220:113426.

17. Ebrahimipour SY, Mirzaei M, Zamani K, Mohamadi M, Bahraman AG, Ramezanpour S. Characterization and *in-vitro* release of coumarin from folic acid-conjugated mesoporous silica for targeted cancer therapy. J Mol Struct. 2025; 1330:141502.

18. Alallam B, Abdkadir E, Hayati A, Keong YY, Lim V. Alginate coated mesoporous silica nanoparticles as oral delivery carrier of curcumin and quercetin to colon cancer: preparation, optimization, characterization, and anticancer activity. Drug Deliv Translat Res 2025;15:1–42.

19. Zahedi P, Ebrahimnejad P, Seyedabadi M, Babaei A. Optimized mesoporous silica nanoparticles for delivery of curcumin and quercetin: enhanced skin permeation and cytotoxicity against A375 melanoma cells. J Cluster Sci. 2025;36:50.

20. Heydari SR, Ghahremani MH, Atyabi F, Bafkary R, Jaafari MR, Dinarvand R. Aptamer-modified chitosan-capped mesoporous silica nanoparticles for co-delivery of cytarabine and daunorubicin in leukemia. Int J Pharm. 2023;32:123495.

21. Salari-Goharizi F, Mahani M, Sepehrian H, Yoosefian M, Khakbaz F. Multifunctional nanocarriers: enhanced doxorubicin release from CQD-tagged SBA-15 silica nanoparticles. J Cluster Sci. 2025:1–12.

22. Ostrowska S, Szukowska M, Kim S, Kim Y, Wawrzyniak D, Mrówczyński R. Doxorubicin and Sorafenib release from mesoporous silica nanoparticles coated with polydopamineinfluence of mechanical and chemical stimuli on the process. Front Coat Dyes Interface Eng. 2025;3:1531144.

23. Hsu TI, Chen YP, Zhang RL, Chen ZA, Wu CH, Chang WC, *et al.* Overcoming the blood–brain tumor barrier with docetaxel-loaded mesoporous silica nanoparticles for treatment of temozolomide-resistant glioblastoma. ACS Appl Mater Interfaces. 2024;16:21722–35.

24. Viswanathan TM, Chitradevi K, Zochedh A, Vijayabhaskar R, Sukumaran S, Kunjiappan S, *et al.* Guanidine–curcumin complex-loaded amine-functionalised hollow mesoporous silica nanoparticles for breast cancer therapy. Cancers. 2022;14:3490.

25. Liu X, Situ A, Kang Y, Villabroza KR, Liao Y, Chang CH, *et al.* Irinotecan delivery by lipid-coated mesoporous silica nanoparticles shows improved efficacy and safety over liposomes for pancreatic cancer. ACS nano. 2016;10:2702–15.

26. Wang X, Xu T, Song H, Zhou L, Li X, Li G, *et al.* Fe3O4-viral-like mesoporous silica nanoparticle (Fe3O4-vMSN)-sustained release

27. of lenvatinib for targeted treatment of hepatocellular carcinoma. Current Cancer Drug Targets. 2025;25:NA.

27. Jafarpour N, Nikpassand M, Faramarzi M. Conjugation of folic acid onto poly (acrylic acid-co-allylamine)-grafted mesoporous silica nanoparticles for controlled methotrexate delivery. J Drug Deliv Sci Technol. 2024;96:105667.

28. Liu Y, Yu S, Jiang X, Wu Q, Shen W, Zou Z, *et al.* Functional paclitaxel-manganese-doped mesoporous silica nanoparticles for orthotopic brain glioma targeted therapy. Mater Design. 2024;238:112715.

29. Shahbaz S, Esmaeili M, Nasab MHF, Imani Z, Bafkary R, Amini M, *et al.* PEGylated mesoporous silica core–shell redox-responsive nanoparticles for delivering paclitaxel to breast cancer cells. Int J Pharm 2024;655:124024.

30. Knežević NŽ, Mrđanović J, Borišev I, Milenković S, Janaćković Đ, Cunin F, *et al.* Hydroxylated fullerene-capped, vinblastine-loaded folic acid-functionalized mesoporous silica nanoparticles for targeted anticancer therapy. RSC Adv. 2016;6:7061–5.

31. Zhao H, Li Y, Chen J, Zhang J, Yang Q, Cui J, *et al.* Environmental stimulus-responsive mesoporous silica nanoparticles as anticancer drug delivery platforms. Colloids Surfaces B: Biointerfaces. 2024;234:113758.

32. Li T, Shi S, Goel S, Shen X, Xie X, Chen Z, *et al.* Recent advancements in mesoporous silica nanoparticles towards therapeutic applications for cancer. Acta Biomater. 2019;89:1–13.

33. Dutta Gupta Y, Mackeyev Y, Krishnan S, Bhandary S. Mesoporous silica nanotechnology: promising advances in augmenting cancer theranostics. Cancer Nanotechnol. 2024;15:9.

34. Asefa T, Tao Z. Biocompatibility of mesoporous silica nanoparticles. Chem Res Toxicol. 2012;25:2265–84.

35. Farjadian F, Roointan A, Mohammadi-Samani S, Hosseini M. Mesoporous silica nanoparticles: synthesis, pharmaceutical applications, biodistribution, and biosafety assessment. Chem Eng J. 2019;359:684–705.

36. Huang Y, Li P, Zhao R, Zhao L, Liu J, Peng S, *et al.* Silica nanoparticles: biomedical applications and toxicity. Biomed Pharmacother. 2022;151:113053.

37. Ghobadi M, Salehi S, Ardestani MTS, Mousavi-Khattat M, Shakeran Z, Khosravi A, *et al.* Amine-functionalized mesoporous silica nanoparticles decorated by silver nanoparticles for delivery of doxorubicin in breast and cervical cancer cells. Euro J Pharm Biopharm. 2024;201:114349.

38. Liao T, Liu C, Wu X, Liu J, Yu W, Xu Z, *et al.* Degradable mesoporous silica nanoparticle/peptide-based "Trojan Horse"-like drug delivery system for seep intratumoral penetration and cancer therapy. ACS Appl Nano Mater. 2024;7:9518–31.

39. Wu H, Ding X, Chen Y, Cai Y, Yang Z, Jin J. EGFR-targeted humanized single chain antibody fragment functionalized silica nanoparticles for precision therapy of cancer. Int J Biol Macromol. 2023;253:127538.

40. Bhartiya P, Chawla R, Dutta PK. Folate receptor targeted chitosan and polydopamine coated mesoporous silica nanoparticles for photothermal therapy and drug delivery. J Macromol Sci Part A. 2022;59:810–7.

41. Akram Z, Daood U, Aati S, Ngo H, Fawzy AS. Formulation of pH-sensitive chlorhexidine-loaded/mesoporous silica nanoparticles modified experimental dentin adhesive. Mater Sci Eng C. 2021;122:111894.

42. Feng H, Li M, Xing Z, Ouyang XK, Ling J. Efficient delivery of fucoxanthin using metal–polyphenol network-coated magnetic mesoporous silica. J Drug Deliv Sci Technol. 2022;77:103842.

43. Slapak EJ, El Mandili M, Ten Brink MS, Kros A, Bijlsma MF, Spek CA. CAPN2-responsive mesoporous silica nanoparticles: a promising nanocarrier for targeted therapy of pancreatic cancer. Cancer Lett. 2024;590:216845.

44. Sreeharsha N, Philip M, Krishna SS, Viswanad V, Sahu RK, Shiroorkar PN, *et al.* Multifunctional mesoporous silica nanoparticles for oral drug delivery. Coatings. 2022;12:358.

45. Priyan SR, Kumar GS, Surendhiran S, Shkir M. Size-controlled synthesis of mesoporous silica nanoparticles using rice husk by microwave-assisted sol–gel method. Int J Appl Ceramic Technol. 2023;20(5):2807–16.

46. Khaliq NU, Lee J, Kim J, Kim Y, Yu S, Kim J, *et al.* Mesoporous silica nanoparticles as a gene delivery platform for cancer therapy. Pharmaceutics. 2023;15:1432.

47. Narayan R, Nayak UY, Raichur AM, Garg S. Mesoporous silica nanoparticles: a comprehensive review on synthesis and recent advances. Pharmaceutics. 2018;10:118.

48. Soundharraj P, Dhinasekaran D, Rakkesh Rajendran A, Prakasarao A, Ganesan S. Investigation on the drug loading efficacy of protoporphyrin functionalized silica precursors (Tetraethyl orthosilicate: TEOS and Biomass silica) for enhanced delivery of 5-fluorouracil. Chem Select. 2023;8:e202204498.

49. Rajput S, Vadia N, Mahajan M. Role of mesoporous silica nanoparticles as drug carriers: evaluation of diverse mesoporous material nanoparticles as potential host for various applications. Adv Funct Porous Mater From Macro to Nano Scale Lengths. 2022:205–34.

50. Semeykina V, Zharov I. Medium controlled aggregative growth as a key step in mesoporous silica nanoparticle formation. J Colloid Interface Sci 2022;615:236–47.

51. Pal N, Lee JH, Cho EB. Recent trends in morphology-controlled synthesis and application of mesoporous silica nanoparticles. Nanomaterials. 2020;10:2122.

52. Kaur A, Bajaj B, Kaushik A, Saini A, Sud D. A review on template assisted synthesis of multi-functional metal oxide nanostructures: status and prospects. Mater Sci Eng B. 2022;286:116005.

53. Hwang J, Lee JH, Chun J. Facile approach for the synthesis of spherical mesoporous silica nanoparticles from sodium silicate. Mater Lett. 2021;283:128765.

54. Lv X, Zhang L, Xing F, Lin H. Controlled synthesis of monodispersed mesoporous silica nanoparticles: particle size tuning and formation mechanism investigation. Microporous Mesoporous Mater. 2016;225:238–44.

55. Zhou C, Yan C, Zhao J, Wang H, Zhou Q, Luo W. Rapid synthesis of morphology-controlled mesoporous silica nanoparticles from silica fume. J Taiwan Inst Chem Eng. 2016;62:307–12.

56. Abburi A, Ali M, Moriya PV. Synthesis of mesoporous silica nanoparticles from waste hexafluorosilicic acid of fertilizer industry. J Mater Res Technol. 2020;9:8074–80.

57. Mohamad DF, Osman NS, Nazri MKHM, Mazlan AA, Hanafi MF, Esa YAM, *et al.* Synthesis of mesoporous silica nanoparticle from banana peel ash for removal of phenol and methyl orange in aqueous solution. Mater Today Proc. 2019;19:1119–25.

58. Li H, Wu X, Yang B, Li J, Xu L, Liu H, *et al.* Evaluation of biomimetically synthesized mesoporous silica nanoparticles as drug carriers: structure, wettability, degradation, biocompatibility and brain distribution. Mat Sci Eng C. 2019;94:453–64.

59. Li Q, Zhou Y. Brief history, preparation method, and biological application of mesoporous silica molecular sieves: a narrative review. Molecules. 2023;28:2013.

60. Gurung S, Gucci F, Cairns G, Chianella I, Leighton GJ. Hollow silica nano and micro spheres with polystyrene templating: a mini-review. Materials. 2022;15:8578.

61. Munir T, Mahmood A, Peter N, Rafaqat N, Imran M, Ali HE. Structural, morphological and optical properties at various concentration of Ag doped SiO2-NPs via sol gel method for antibacterial and anticancer activities. Surf Interfaces. 2023;38:102759.

62. Porrang S, Rahemi N, Davaran S, Mahdavi M, Hassanzadeh B. Synthesis of temperature/pH dual-responsive mesoporous silica nanoparticles by surface modification and radical polymerization for anti-cancer drug delivery. Colloids Surf A: Physicochem Eng Aspects. 2021;623:126719.

63. Choudante PC, Mamilla J, Kongari L, Díaz-García D, Prashar S, Gómez-Ruiz S, *et al.* Functionalized tin-loaded mesoporous silica nanoparticles for targeted therapy of triple-negative breast cancer: evaluation of cytogenetic toxicity. J Drug Deliv Sci Technol. 2024;94:105502.

64. Sun T, Li C, Li X, Song H, Su B, You H, *et al.* Pharmaceutical Nanotechnology. In Nanomedicine. Springer; 2023. pp 179–283.

65. Xiang L, Li Q, Li C, Yang Q, Xu F, Mai Y. Block copolymer self-assembly directed synthesis of porous materials with ordered bicontinuous structures and their potential applications. Adv Mater. 2023;35:2207684.

66. Florensa M, Llenas M, Medina-Gutiérrez E, Sandoval S, Tobías-Rossell G. Key parameters for the rational design, synthesis, and functionalization of biocompatible mesoporous silica nanoparticles. Pharmaceutics. 2022;14:2703.

67. Zhang L, Jin L, Liu B, He J. Templated growth of crystalline mesoporous materials: from soft/hard templates to colloidal templates. Front Chem. 2019;7:22.

68. Jin L, Liu B, Louis ME, Li G, He J. Highly crystalline mesoporous titania loaded with monodispersed gold nanoparticles: controllable metal–support interaction in porous materials. ACS Appl Mater Interfaces. 2020;12:9617–27.

69. Mohanan S, Sathish C, Ramadass K, Liang M, Vinu A. Design and synthesis of cabazitaxel loaded core-shell mesoporous silica nanoparticles with different morphologies for prostate cancer therapy. Small. 2024;20:2303269.

70. AlMohaimadi KM, Albishri HM, Thumayri KA, AlSuhaimi AO, Mehdar YT, Hussein BH. Facile hydrothermal assisted basic catalyzed sol gel synthesis for mesoporous silica nanoparticle from alkali silicate solutions using dual structural templates. Gels. 2024;10:839.

71. Shakeran Z, Keyhanfar M, Varshosaz J, Sutherland DS. Biodegradable nanocarriers based on chitosan-modified mesoporous silica nanoparticles for delivery of methotrexate for application in breast cancer treatment. Mater Sci Eng C. 2021;118:111526.

72. Bilal M, Iqbal HM, Adil SF, Shaik MR, Abdelgawad A, Hatshan MR, *et al.* Surface-coated magnetic nanostructured materials for robust bio-catalysis and biomedical applications-a review. J Adv Res. 2022;38:157–77.

73. Marques A, Costa P, Velho S, Amaral M. Functionalizing nanoparticles with cancer-targeting antibodies: a comparison of strategies. J Controlled Release. 2020;320:180–200.

74. Xu X, Li H, Li K, Zeng Q, Liu Y, Zeng Y, *et al.* A photo-triggered conjugation approach for attaching RGD ligands to biodegradable mesoporous silica nanoparticles for the tumor fluorescent imaging. Nanomedicine Nanotechnol Biol Med. 2019;19:136–44.

75. Alfhaid LHK. Recent advance in functionalized mesoporous silica nanoparticles with stimuli-responsive polymer brush for controlled drug delivery. Soft Mater. 2022;20:364–78.

76. Li QL, Sun Y, Sun YL, Wen J, Zhou Y, Bing QM, *et al.* Mesoporous silica nanoparticles coated by layer-by-layer self-assembly using cucurbit [7] uril for *in vitro* and *in vivo* anticancer drug release. Chem Mater. 2014;26:6418–31.

77. Wei Y, Gao L, Wang L, Shi L, Wei E, Zhou B, et al. Polydopamine and peptide decorated doxorubicin-loaded mesoporous silica nanoparticles as a targeted drug delivery system for bladder cancer therapy. Drug Deliv. 2017;24:681-91.

78. Zoppe JO, Ataman NC, Mocny P, Wang J, Moraes J, Klok HA. Surface-initiated controlled radical polymerization: state-of-the-art, opportunities, and challenges in surface and interface engineering with polymer brushes. Chem Rev. 2017;117:1105–318.

79. Huang R, Shen YW, Guan YY, Jiang YX, Wu Y, Rahman K, *et al.* Mesoporous silica nanoparticles: facile surface functionalization and versatile biomedical applications in oncology. Acta Biomater. 2020;116:1–15.

80. Abu-Dief AM, Alsehli M, Al-Enizi A, Nafady A. Recent advances in mesoporous silica nanoparticles for targeted drug delivery applications. Curr Drug Deliv. 2022;19:436–50.

81. Lu J, Luo B, Chen Z, Yuan Y, Kuang Y, Wan L, *et al.* Host-guest fabrication of dual-responsive hyaluronic acid/mesoporous silica nanoparticle based drug delivery system for targeted cancer therapy. Int J Biol Macromol. 2020;146:363–73.

82. Noreen S, Maqbool A, Maqbool I, Shafique A, Khan MM, Junejo Y, *et al.* Multifunctional mesoporous silica-based nanocomposites: synthesis and biomedical applications. Mater Chem Phy. 2022;285:126132.

83. Varache M, Bezverkhyy I, Weber G, Saviot L, Chassagnon R, Baras F, *et al.* Loading of cisplatin into mesoporous silica nanoparticles: effect of surface functionalization. Langmuir. 2019;35:8984–95.

84. Wani A, Muthuswamy E, Savithra GHL, Mao G, Brock S, Oupický D. Surface functionalization of mesoporous silica nanoparticles controls loading and release behavior of mitoxantrone. Pharm Res. 2012;29:2407–18.

85. Chang B, Guo J, Liu C, Qian J, Yang W. Surface functionalization of magnetic mesoporous silica nanoparticles for controlled drug release. J Mater Chem. 2010;20:9941–7.

86. She X, Chen L, Li C, He C, He L, Kong L. Functionalization of hollow mesoporous silica nanoparticles for improved 5-FU loading. J Nanomater. 2015;16:108.

87. Bahrami Z, Badiei A, Atyabi F, Darabi HR, Mehravi B. Piperazine and its carboxylic acid derivatives-functionalized mesoporous silica as nanocarriers for gemcitabine: adsorption and release study. Mater Sci Eng C. 2015;49:66–74.

88. Niroumand U, Firouzabadi N, Goshtasbi G, Hassani B, Ghasemiyeh P, Mohammadi-Samani S. The effect of size, morphology and surface properties of mesoporous silica nanoparticles on pharmacokinetic aspects and potential toxicity concerns. Front Mater. 2023;10:1189463.

89. Yang B, Zhou S, Zeng J, Zhang L, Zhang R, Liang K, *et al.* Super-assembled core-shell mesoporous silica-metal-phenolic network nanoparticles for combinatorial photothermal therapy and chemotherapy. Nano Res. 2020;13:1013–9.

90. Yang G, Li Z, Wu F, Chen M, Wang R, Zhu H, *et al.* Improving solubility and bioavailability of breviscapine with mesoporous silica nanoparticles prepared using ultrasound-assisted solution-enhanced dispersion by supercritical fluids method. Int J Nanomedicine. 2020;15:1661–75.

91. Gisbert-Garzarán M, Manzano M, Vallet-Regí M. Mesoporous silica nanoparticles for the treatment of complex bone diseases: bone cancer, bone infection and osteoporosis. Pharmaceutics. 2020;12:83.

92. Peng S, Yuan X, Lin W, Cai C, Zhang L. pH-responsive controlled release of mesoporous silica nanoparticles capped with Schiff base copolymer gatekeepers: experiment and molecular dynamics simulation. Colloids Surf B Biointerfaces. 2019;176:394–403.

93. Guo F, Li G, Zhou H, Ma S, Guo L, Liu X. Temperature and H2O2-operated nano-valves on mesoporous silica nanoparticles for controlled drug release and kinetics. Colloids Surf B Biointerf. 2020;187:110643.

94. Huang P, Lian D, Ma H, Gao N, Zhao L, Luan P, *et al.* New advances in gated materials of mesoporous silica for drug controlled release. Chinese Chem Lett. 2021;32:3696–704.

95. Kankala RK, Han YH, Na J, Lee CH, Sun Z, Wang SB, *et al.* Nanoarchitectured structure and surface biofunctionality of mesoporous silica nanoparticles. Adv Mater. 2020;32:1907035.

96. Lu H, Zhao Q, Wang X, Mao Y, Chen C, Gao Y, *et al.* Multi-stimuli responsive mesoporous silica-coated carbon nanoparticles for chemo-photothermal therapy of tumor. Colloids Surf B Biointerfaces. 2020;190:110941.

97. Li T, Shen X, Geng Y, Chen Z, Li L, Li S, *et al.* Folate-functionalized magnetic-mesoporous silica nanoparticles for drug/gene codelivery to potentiate the antitumor efficacy. ACS Appl Mater Interfaces. 2016;8:13748–58.

98. Wang T, Wang M, Ding C, Fu J. Mono-benzimidazole functionalized β-cyclodextrins as supramolecular nanovalves for pH-triggered release of p-coumaric acid. Chem Commun. 2014;50:12469–72.

99. Du L, Song H, Liao S. A biocompatible drug delivery nanovalve system on the surface of mesoporous nanoparticles. Microporous Mesoporous Mater. 2012;147:200–4.

100. Chen H, Kuang Y, Liu R, Chen Z, Jiang B, Sun Z, *et al.* Dual-pH-sensitive mesoporous silica nanoparticle-based drug delivery system for tumor-triggered intracellular drug release. J Mater Sci. 2018;53:10653–65.

101. Eskandari P, Bigdeli B, Porgham Daryasari M, Baharifar H, Bazri B, Shourian M, *et al.* Gold-capped mesoporous silica nanoparticles as an excellent enzyme-responsive nanocarrier for controlled doxorubicin delivery. J Drug Targeting. 2019;27:1084–93.

102. Mondragón L, Mas N, Ferragud V, de la Torre C, Agostini A, Martínez-Máñez R, *et al.* Enzyme-responsive intracellular-controlled release using silica mesoporous nanoparticles capped with ε-Poly-L-lysine. Chem–A Eur J. 2014;20:5271–81.

103. Saroj S, Rajput SJ. Etoposide encapsulated functionalized mesoporous silica nanoparticles: Synthesis, characterization and effect of functionalization on dissolution kinetics in simulated and biorelevant media. J Drug Deliv Sci Technol. 2018;44:27–40.

104. Thi TTH, Nguyen TNQ, Hoang DT, Nguyen DH. Functionalized mesoporous silica nanoparticles and biomedical applications. Mater Sci Eng C. 2019;99:631–56.

105. Kim EC, Ou W, Dai Phung C, Nguyen TT, Pham TT, Poudel K, *et al.* Targeting and clearance of senescent foamy macrophages and senescent endothelial cells by antibody-functionalized mesoporous silica nanoparticles for alleviating aorta atherosclerosis. Biomaterials. 2021;269:120677.

106. Shadmani N, Makvandi P, Parsa M, Azadi A, Nedaei K, Mozafari N, *et al.* Enhancing methotrexate delivery in the brain by mesoporous silica nanoparticles functionalized with cell-penetrating peptide using *in vivo* and *ex vivo* monitoring. Mol Pharm. 2023;20:1531–48.

107. Sakhtianchi R, Darvishi B, Mirzaie Z, Dorkoosh F, Shanehsazzadeh S, Dinarvand R. Pegylated magnetic mesoporous silica nanoparticles decorated with AS1411 Aptamer as a targeting delivery system for cytotoxic agents. Pharm Dev Technol. 2019;24:1063–75.

108. Chen C, Tang W, Jiang D, Yang G, Wang X, Zhou L, *et al.* Hyaluronic acid conjugated polydopamine functionalized mesoporous silica nanoparticles for synergistic targeted chemo-photothermal therapy. Nanoscale. 2019;11:11012–24.

109. Rosenholm JM, Sahlgren C, Lindén M. Towards multifunctional, targeted drug delivery systems using mesoporous silica nanoparticles–opportunities & challenges. Nanoscale. 2010;2:1870–83.

110. Liu Y, Dai R, Wei Q, Li W, Zhu G, Chi H, *et al.* Dual-functionalized janus mesoporous silica nanoparticles with active targeting and charge reversal for synergistic tumor-targeting therapy. ACS Appl Mater Interfaces. 2019;11:44582–92.

111. Barui S, Cauda V. Multimodal decorations of mesoporous silica nanoparticles for improved cancer therapy. Pharmaceutics. 2020;12:527.

112. Chen L, She X, Wang T, He L, Shigdar S, Duan W, *et al.* Overcoming acquired drug resistance in colorectal cancer cells by targeted delivery of 5-FU with EGF grafted hollow mesoporous silica nanoparticles. Nanoscale. 2015;7:14080–92.

113. Liu K, Wang ZQ, Wang S-J, Liu P, Qin Y-H, Ma Y, *et al.* Hyaluronic acid-tagged silica nanoparticles in colon cancer therapy: therapeutic efficacy evaluation. Int J Nanomedicine. 2015;10:6445–54.

114. Radhakrishnan K, Tripathy J, Datey A, Chakravortty D, Raichur AM. Mesoporous silica–chondroitin sulphate hybrid nanoparticles for targeted and bio-responsive drug delivery. New J Chem. 2015;39:1754–60.

115. Xie X, Li F, Zhang H, Lu Y, Lian S, Lin H, *et al.* EpCAM aptamer-functionalized mesoporous silica nanoparticles for efficient colon cancer cell-targeted drug delivery. Eur J Pharm Sci. 2016;83:28–35.

116. Chen X, Sun H, Hu J, Han X, Liu H, Hu Y. Transferrin gated mesoporous silica nanoparticles for redox-responsive and targeted drug delivery. Colloids Surf B Biointerfaces. 2017;152:77–84.

117. Khosravian P, Shafiee Ardestani M, Khoobi M, Ostad SN, Dorkoosh FA, Akbari Javar H, *et al.* Mesoporous silica nanoparticles functionalized with folic acid/methionine for active targeted delivery of docetaxel. OncoTargets Ther. 2016;9:7315–30.

118. Quan G, Pan X, Wang Z, Wu Q, Li G, Dian L, *et al.* Lactosaminated mesoporous silica nanoparticles for asialoglycoprotein receptor targeted anticancer drug delivery. J Nanobiotechnol. 2015;13:1–12.

119. Sarkar A, Ghosh S, Chowdhury S, Pandey B, Sil PC. Targeted delivery of quercetin loaded mesoporous silica nanoparticles to the breast cancer cells. Biochim Biophys Acta (BBA)-Gen Subjects. 2016;1860:2065–75.

120. Murugan C, Rayappan K, Thangam R, Bhanumathi R, Shanthi K, Vivek R, *et al.* Combinatorial nanocarrier based drug delivery approach for amalgamation of anti-tumor agents in breast cancer cells: an improved nanomedicine strategy. Sci Rep. 2016;6:34053.

121. Goel S, Chen F, Hong H, Valdovinos HF, Hernandez R, Shi S, *et al.* VEGF121-conjugated mesoporous silica nanoparticle: a tumor targeted drug delivery system. ACS Appl Mater Interfaces. 2014;6:21677–85.

122. Rivero-Buceta E, Vidaurre-Agut C, Vera-Donoso CsD, Benlloch JM, Moreno-Manzano V, Botella P. PSMA-targeted mesoporous silica nanoparticles for selective intracellular delivery of docetaxel in prostate cancer cells. ACS Omega. 2019;4:1281–91.

123. Kumar B, Kulanthaivel S, Mondal A, Mishra S, Banerjee B, Bhaumik A, *et al.* Mesoporous silica nanoparticle based enzyme responsive system for colon specific drug delivery through guar gum capping. Colloids Surf B Biointerfaces. 2017;150:352–61.

124. Cui Y, Xu Q, Chow PKH, Wang D, Wang CH. Transferrin-conjugated magnetic silica PLGA nanoparticles loaded with doxorubicin and paclitaxel for brain glioma treatment. Biomaterials. 2013;34:8511–20.

125. Mo J, He L, Ma B, Chen T. Tailoring particle size of mesoporous silica nanosystem to antagonize glioblastoma and overcome blood–brain barrier. ACS Appl Mater Interfaces. 2016;8:6811–25.

126. Chi X, Zhang R, Zhao T, Gong X, Wei R, Yin Z, *et al.* Targeted arsenite-loaded magnetic multifunctional nanoparticles for treatment of hepatocellular carcinoma. Nanotechnology. 2019;30:175101.

127. Liu CM, Chen GB, Chen HH, Zhang JB, Li HZ, Sheng MX, *et al.* Cancer cell membrane-cloaked mesoporous silica nanoparticles with a pH-sensitive gatekeeper for cancer treatment. Colloids Surf B Biointerfaces. 2019;175:477–86.

128. Tan J, Yang N, Zhong L, Tan J, Hu Z, Zhao Q, *et al.* A new theranostic system based on endoglin aptamer conjugated fluorescent silica nanoparticles. Theranostics. 2017;7:4862.

129. Vallet-Regí M, Schüth F, Lozano D, Colilla M, Manzano M. Engineering mesoporous silica nanoparticles for drug delivery: where are we after two decades? Chem Soc Rev. 2022;51:5365–451.

130. Garrido-Cano I, Candela-Noguera V, Herrera G, Cejalvo JM, Lluch A, Marcos MD, *et al.* Biocompatibility and internalization assessment of bare and functionalised mesoporous silica nanoparticles. Microporous Mesoporous Mater. 2021;310:110593.

131. Taleghani AS, Nakhjiri AT, Khakzad MJ, Rezayat SM, Ebrahimnejad P, Heydarinasab A, *et al.* Mesoporous silica nanoparticles as a versatile nanocarrier for cancer treatment: a review. J Mol Liquids. 2021;328:115417.

132. Hosseinpour S, Walsh LJ, Xu C. Biomedical application of mesoporous silica nanoparticles as delivery systems: a biological safety perspective. J Mater Chem B. 2020;8:9863–76.

133. Ahmadi F, Sodagar-Taleghani A, Ebrahimnejad P, Moghaddam SPH, Ebrahimnejad F, Asare-Addo K, *et al.* A review on the latest developments of mesoporous silica nanoparticles as a promising platform for diagnosis and treatment of cancer. Int J Pharm. 2022;625:122099.

134. Zhou S, Zhong Q, Wang Y, Hu P, Zhong W, Huang CB, *et al.* Chemically engineered mesoporous silica nanoparticles-based intelligent delivery systems for theranostic applications in multiple cancerous/non-cancerous diseases. Coordination Chem Rev. 2022;452:214309.

135. Heidari R, Khosravian P, Mirzaei SA, Elahian F. siRNA delivery using intelligent chitosan-capped mesoporous silica nanoparticles for overcoming multidrug resistance in malignant carcinoma cells. Sci Rep. 2021;11:20531.

136. Hashemzadeh N, Dolatkhah M, Aghanejad A, Barzegar-Jalali M, Omidi Y, Adibkia K, *et al.* Folate receptor-mediated delivery of 1-MDT-loaded mesoporous silica magnetic nanoparticles to target breast cancer cells. Nanomedicine. 2021;16:2137–54.

137. Rastegari E, Hsiao YJ, Lai WY, Lai YH, Yang TC, Chen SJ, *et al.* An update on mesoporous silica nanoparticle applications in nanomedicine. Pharmaceutics. 2021;13:1067.

138. Zhu J, Zhang Y, Chen X, Zhang Y, Zhang K, Zheng H, *et al.* Angiopep-2 modified lipid-coated mesoporous silica nanoparticles for glioma targeting therapy overcoming BBB. Biochem Biophys Res Commun. 2021;534:902–7

139. To KK, Wu M, Tong CW, Yan W. Drug transporters in the development of multidrug resistance in colorectal cancer. In Drug resistance in colorectal cancer: molecular mechanisms and therapeutic strategies. San Diego, CA: Elsevier; 2020. pp 35–55

140. Kankala RK, Liu CG, Chen AZ, Wang SB, Xu PY, Mende LK, *et al.* Overcoming multidrug resistance through the synergistic effects of hierarchical pH-sensitive, ROS-generating nanoreactors. ACS Biomater Sci Eng. 2017;3:2431–42.

141. Fang J, Zhang S, Xue X, Zhu X, Song S, Wang B, *et al.* Quercetin and doxorubicin co-delivery using mesoporous silica nanoparticles enhance the efficacy of gastric carcinoma chemotherapy. Int J Nanomedicine. 2018;13:5113–26.

142. Zhai Y, Su J, Ran W, Zhang P, Yin Q, Zhang Z, *et al.* Preparation and application of cell membrane-camouflaged nanoparticles for cancer therapy. Theranostics. 2017;7:2575.

143. Su J, Sun H, Meng Q, Zhang P, Yin Q, Li Y. Enhanced blood suspensibility and laser-activated tumor-specific drug release of theranostic mesoporous silica nanoparticles by functionalizing with erythrocyte membranes. Theranostics. 2017;7:523.

144. Tamarov K, Näkki S, Xu W, Lehto VP. Approaches to improve the biocompatibility and systemic circulation of inorganic porous nanoparticles. J Mater Chem B. 2018;6:3632–49.

145. Xuan M, Shao J, Dai L, He Q, Li J. Macrophage cell membrane camouflaged mesoporous silica nanocapsules for *in vivo* cancer therapy. Adv Healthcare Mater. 2015;4:1645–52.

146. Yue J, Wang Z, Shao D, Chang Z, Hu R, Li L, *et al.* Cancer cell membrane-modified biodegradable mesoporous silica nanocarriers for berberine therapy of liver cancer. RSC Adv. 2018;8:40288–97.

147. Babaei M, Abnous K, Taghdisi SM, Taghavi S, Saljooghi AS, Ramezani M, *et al.* Targeted rod-shaped mesoporous silica nanoparticles for the co-delivery of camptothecin and survivin shRNA in to colon adenocarcinoma *in vitro* and *in vivo*. Eur J Pharm Biopharm. 2020;156:84–96.

148. Zhang J, Shen B, Chen L, Chen L, Meng Y, Feng J. A dual-sensitive mesoporous silica nanoparticle based drug carrier for cancer synergetic therapy. Colloids Surf B Biointerfaces. 2019;175:65–72.

149. Sun L, Wang D, Chen Y, Wang L, Huang P, Li Y, *et al.* Core-shell hierarchical mesostructured silica nanoparticles for gene/chemo-synergetic stepwise therapy of multidrug-resistant cancer. Biomaterials. 2017;133:219–28.

150. Wang C, Wu L, Yuan H, Yu H, Xu J, Chen S, *et al.* A powerful antitumor "trident": the combination of radio-, immuno-and anti-

angiogenesis therapy based on mesoporous silica single coated gold nanoparticles. J Mater Chem B. 2023;11:879–89.

151. Meng H, Wang M, Liu H, Liu X, Situ A, Wu B, *et al.* Use of a lipid-coated mesoporous silica nanoparticle platform for synergistic gemcitabine and paclitaxel delivery to human pancreatic cancer in mice. ACS Nano. 2015;9:3540–57.

152. Jia L, Li Z, Shen J, Zheng D, Tian X, Guo H, *et al.* Multifunctional mesoporous silica nanoparticles mediated co-delivery of paclitaxel and tetrandrine for overcoming multidrug resistance. Int J Pharm. 2015;489:318–30.

153. Li S, Zhang Y, He XW, Li WY, Zhang YK. Multifunctional mesoporous silica nanoplatform based on silicon nanoparticles for targeted two-photon-excited fluorescence imaging-guided chemo/photodynamic synergetic therapy *in vitro*. Talanta. 2020;209:120552.

154. Wang J, Zhang Y, Liu L, Cui Z, Liu X, Wang L, *et al.* Combined chemo/photothermal therapy based on mesoporous silica-Au core-shell nanoparticles for hepatocellular carcinoma treatment. Drug Dev Indus Pharm. 2019;45(9):1487–95.

155. Pan G, Jia TT, Huang Q-X, Qiu Y-Y, Xu J, Yin P-H, *et al.* Mesoporous silica nanoparticles (MSNs)-based organic/inorganic hybrid nanocarriers loading 5-Fluorouracil for the treatment of colon cancer with improved anticancer efficacy. Colloids Surf B Biointerfaces. 2017;159:375–85.

156. Narayan R, Gadag S, Cheruku SP, Raichur AM, Day CM, Garg S, *et al.* Chitosan-glucuronic acid conjugate coated mesoporous silica nanoparticles: a smart pH-responsive and receptor-targeted system for colorectal cancer therapy. Carbohydrate Poly. 2021;261:117893.

157. Martínez-Edo G, Fornaguera C, Borrós S, Sánchez-García D. Glycyrrhetinic acid-functionalized mesoporous silica nanoparticles for the co-delivery of DOX/CPT-PEG for targeting HepG2 cells. Pharmaceutics. 2020;12:1048.

158. Moghadam ME, Sadeghi M, Mansouri-Torshizi H, Saidifar M. High cancer selectivity and improving drug release from mesoporous silica nanoparticles in the presence of human serum albumin in cisplatin, carboplatin, oxaliplatin, and oxalipalladium treatment. Eur J Pharm Sci. 2023;187:106477.

159. Busa P, Kankala RK, Deng JP, Liu CL, Lee CH. Conquering cancer multi-drug resistance using curcumin and cisplatin prodrug-encapsulated mesoporous silica nanoparticles for synergistic chemo- and photodynamic therapies. Nanomaterials. 2022;12:3693.

160. Zhao P, Qiu L, Zhou S, Li L, Qian Z, Zhang H. Cancer cell membrane camouflaged mesoporous silica nanoparticles combined with immune checkpoint blockade for regulating tumor microenvironment and enhancing antitumor therapy. Int J Nanomedicine. 2021;16:2107–21.

161. Hao Y, Zheng C, Song Q, Chen H, Nan W, Wang L, *et al.* Pressure-driven accumulation of Mn-doped mesoporous silica nanoparticles containing 5-aza-2-deoxycytidine and docetaxel at tumours with a dry cupping device. J Drug Targeting. 2021;29:900–9.

162. Wang D, Huang J, Wang X, Yu Y, Zhang H, Chen Y, *et al.* The eradication of breast cancer cells and stem cells by 8-hydroxyquinoline-loaded hyaluronan modified mesoporous silica nanoparticle-supported lipid bilayers containing docetaxel. Biomaterials. 2013;34:7662–73.

163. Yan J, Xu X, Zhou J, Liu C, Zhang L, Wang D, *et al.* Fabrication of a pH/redox-triggered mesoporous silica-based nanoparticle with microfluidics for anticancer drugs doxorubicin and paclitaxel codelivery. ACS Appl Bio Mater. 2020;3:1216–25.

164. Saini K, Bandyopadhyaya R. Transferrin-conjugated polymer-coated mesoporous silica nanoparticles loaded with gemcitabine for killing pancreatic cancer cells. ACS Appl Nano Mater. 2019;3:229–40.

165. Brezoiu AM, Prelipcean AM, Lincu D, Deaconu M, Vasile E, Tatia R, *et al.* Nanoplatforms for irinotecan delivery based on mesoporous silica modified with a natural polysaccharide. Materials. 2022;15:7003.

166. Nie Z, Wang D, Wang S, Wang L. Facile construction of irinotecan loaded mesoporous nano-formulation with surface-initiated polymerization to improve stimuli-responsive drug delivery for breast cancer therapy. Heliyon. 2023;9:e15087.

167. Zhang K, Gao J, Li S, Ma T, Deng L, Kong Y. Construction of a pH-responsive drug delivery platform based on the hybrid of mesoporous silica and chitosan. J Saudi Chem Soc. 2021;25:101174.

168. Salve R, Kumar P, Chaudhari BP, Gajbhiye V. Aptamer tethered bio-responsive mesoporous silica nanoparticles for efficient targeted delivery of paclitaxel to treat ovarian cancer cells. J Pharm Sci. 2023;112:1450–9.

169. Slapak EJ, El Mandili M, Brink MST, Kros A, Bijlsma MF, Spek CA. Preclinical assessment of ADAM9-responsive mesoporous silica nanoparticles for the treatment of pancreatic cancer. Int J Mol Sci. 2023;24:10704.

170. Liu M, Fu M, Yang X, Jia G, Shi X, Ji J, *et al.* Paclitaxel and quercetin co-loaded functional mesoporous silica nanoparticles overcoming multidrug resistance in breast cancer. Colloids Surf B Biointerfaces. 2020;196:111284.

171. Gautam M, Thapa RK, Poudel BK, Gupta B, Ruttala HB, Nguyen HT, *et al.* Aerosol technique-based carbon-encapsulated hollow mesoporous silica nanoparticles for synergistic chemo-photothermal therapy. Acta Biomaterialia. 2019;88:448–61.

172. Setia A, Mehata AK, Malik AK, Viswanadh MK, Muthu MS. Theranostic magnetic nanoparticles: synthesis, properties, toxicity, and emerging trends for biomedical applications. J Drug Deliv Sci Technol. 2023;81:104295.

173. Li X, Zhang X, Zhao Y, Sun L. Fabrication of biodegradable Mn-doped mesoporous silica nanoparticles for pH/redox dual response drug delivery. J Inorgan Biochem. 2020;202:110887.

174. Yu J, Dan N, Eslami SM, Lu X. State of the art of silica nanoparticles: an overview on biodistribution and preclinical toxicity studies. AAPS J. 2024;26:35.

175. Barguilla I, Candela-Noguera V, Oliver P, Annangi B, Díez P, Aznar E, *et al.* Toxicological profiling and long-term effects of bare, PEGylated-and galacto-oligosaccharide-functionalized mesoporous silica nanoparticles. Int J Mol Sci. 2023;24:16158.

176. Li Z, Zhang Y, Feng N. Mesoporous silica nanoparticles: synthesis, classification, drug loading, pharmacokinetics, biocompatibility, and application in drug delivery. Expert Opinion Drug Deliv. 2019;16:219–37.

177. Thapa R, Ali H, Afzal O, Bhat AA, Almalki WH, Alzarea SI, *et al.* Unlocking the potential of mesoporous silica nanoparticles in breast cancer treatment. J Nanoparticle Res. 2023;25:169.

178. Rani R, Malik P, Dhania S, Mukherjee TK. Recent advances in mesoporous silica nanoparticle-mediated drug delivery for breast cancer treatment. Pharmaceutics. 2023;15:227.

179. Bhavsar D, Patel V, Sawant K. Systematic investigation of *in vitro* and *in vivo* safety, toxicity and degradation of mesoporous silica nanoparticles synthesized using commercial sodium silicate. Microporous Mesoporous Mater. 2019;284:343–52.

180. Huang X, Li L, Liu T, Hao N, Liu H, Chen D, *et al.* The shape effect of mesoporous silica nanoparticles on biodistribution, clearance, and biocompatibility *in vivo*. ACS Nano. 2011;5:5390–9.

181. He Q, Shi J. Mesoporous silica nanoparticle based nano drug delivery systems: synthesis, controlled drug release and delivery, pharmacokinetics and biocompatibility. J Mater Chem. 2011;21:5845–55.

182. Gisbert-Garzaran M, Lozano D, Matsumoto K, Komatsu A, Manzano M, Tamanoi F, *et al.* Designing mesoporous silica nanoparticles to overcome biological barriers by incorporating targeting and endosomal escape. ACS Appl Mater Interfaces. 2021;13:9656–66.

183. Lu J, Liong M, Li Z, Zink JI, Tamanoi F. Biocompatibility, biodistribution, and drug-delivery efficiency of mesoporous silica nanoparticles for cancer therapy in animals. Small. 2010;6:1794–805.

184. Deng YD, Zhang XD, Yang XS, Huang ZL, Wei X, Yang XF, *et al.* Subacute toxicity of mesoporous silica nanoparticles to the

intestinal tract and the underlying mechanism. J Hazardous Mater. 2021;409:124502.

185. Mohammadpour R, Cheney DL, Grunberger JW, Yazdimamaghani M, Jedrzkiewicz J, Isaacson KJ, *et al.* One-year chronic toxicity evaluation of single dose intravenously administered silica nanoparticles in mice and their *Ex vivo* human hemocompatibility. J Controlled Release. 2020;324:471–81.

186. Zhang X, Luan J, Chen W, Fan J, Nan Y, Wang Y, *et al.* Mesoporous silica nanoparticles induced hepatotoxicity via NLRP3 inflammasome activation and caspase-1-dependent pyroptosis. Nanoscale. 2018;10:9141–52.

187. Mahmoud AM, Desouky EM, Hozayen WG, Bin-Jumah M, El-Nahass ES, Soliman HA, *et al.* Mesoporous silica nanoparticles trigger liver and kidney injury and fibrosis via altering TLR4/NF-κB, JAK2/STAT3 and Nrf2/HO-1 signaling in rats. Biomolecules. 2019;9:528.

188. Ahmadi A, Sokunbi M, Patel T, Chang MW, Ahmad Z, Singh N. Influence of critical parameters on cytotoxicity induced by mesoporous silica nanoparticles. Nanomaterials. 2022;12:2016.

189. Xu W, Zhou M, Guo Z, Lin S, Li M, Kang Q, *et al.* Impact of macroporous silica nanoparticles at sub-50nm on bio-behaviors and biosafety in drug-resistant cancer models. Colloids Surfaces B: Biointerfaces. 2021;206:111912.

190. Moodley T, Singh M. Polymeric mesoporous silica nanoparticles for enhanced delivery of 5-fluorouracil *in vitro*. Pharmaceutics. 2019;11:288.

191. Li X, Sun W, Zhang Z, Kang Y, Fan J, Peng X. Red light-triggered polyethylene glycol deshielding from photolabile cyanine-modified mesoporous silica nanoparticles for on-demand drug release. ACS Appl Bio Mater. 2020;3:8084–93.

192. Hudson SP, Padera RF, Langer R, Kohane DS. The biocompatibility of mesoporous silicates. Biomaterials. 2008;29:4045–55.

193. Liu T, Li L, Teng X, Huang X, Liu H, Chen D, *et al.* Single and repeated dose toxicity of mesoporous hollow silica nanoparticles in intravenously exposed mice. Biomaterials. 2011;32:1657–68.

194. Abdo GG, Zagho MM, Khalil A. Recent advances in stimuli-responsive drug release and targeting concepts using mesoporous silica nanoparticles. Emerg Mater. 2020;3:407–25.

195. Yan T, He J, Liu R, Liu Z, Cheng J. Chitosan capped pH-responsive hollow mesoporous silica nanoparticles for targeted chemo-photo combination therapy. Carbohydrate Poly. 2020;231:115706.

196. Ghaferi M, Asadollahzadeh MJ, Akbarzadeh A, Ebrahimi Shahmabadi H, Alavi SE. Enhanced efficacy of PEGylated liposomal cisplatin: *in vitro* and *in vivo* evaluation. Int J Mol Sci. 2020;21:559.

197. Gao Y, Gao D, Shen J, Wang Q. A review of mesoporous silica nanoparticle delivery systems in chemo-based combination cancer therapies. Front Chem. 2020;8:598722.

198. Lohiya G, Katti DS. Carboxylated chitosan-mediated improved efficacy of mesoporous silica nanoparticle-based targeted drug delivery system for breast cancer therapy. Carbohydrate Poly. 2022;277:118822.

199. Cordeiro R, Carvalho A, Durães L, Faneca H. Triantennary GalNAc-functionalized multi-responsive mesoporous silica nanoparticles for drug delivery targeted at asialoglycoprotein receptor. Int J Mol Sci. 2022;23:6243.

200. Ong C, Cha BG, Kim J. Mesoporous silica nanoparticles doped with gold nanoparticles for combined cancer immunotherapy and photothermal therapy. ACS Appl Bio Mater. 2019;2:3630–8.

201. Zhu Y, Xu J, Wang Y, Chen C, Gu H, Chai Y, *et al.* Silver nanoparticles-decorated and mesoporous silica coated single-walled carbon nanotubes with an enhanced antibacterial activity for killing drug-resistant bacteria. Nano Res. 2020;13:389–400.

202. Meng H, Xue M, Xia T, Ji Z, Tarn DY, Zink JI, *et al.* Use of size and a copolymer design feature to improve the biodistribution and the enhanced permeability and retention effect of doxorubicin-loaded mesoporous silica nanoparticles in a murine xenograft tumor model. ACS Nano. 2011;5:4131–44.

203. Sivamaruthi BS, Thangaleela S, Kesika P, Suganthy N, Chaiyasut C. Mesoporous silica-based nanoplatforms are theranostic agents for the treatment of inflammatory disorders. Pharmaceutics. 2023;15:439.

204. Li J, Sun R, Xu H, Wang G. Integrative metabolomics, proteomics and transcriptomics analysis reveals liver toxicity of mesoporous silica nanoparticles. Front Pharmacol. 2022;13:835359.

205. Lérida-Viso A, Estepa-Fernández A, García-Fernández A, Martí-Centelles V, Martínez-Máñez R. Biosafety of mesoporous silica nanoparticles; towards clinical translation. Adv Drug Deliv Rev. 2023;201:115049.

206. Bukara K, Schueller L, Rosier J, Martens MA, Daems T, Verheyden L, *et al.* Ordered mesoporous silica to enhance the bioavailability of poorly water-soluble drugs: proof of concept in man. Eur J Pharm Biopharm. 2016;108:220–5.

207. Meola TR, Abuhelwa AY, Joyce P, Clifton P, Prestidge CA. A safety, tolerability, and pharmacokinetic study of a novel simvastatin silica-lipid hybrid formulation in healthy male participants. Drug Deliv Transl Res. 2021;11:1261–72.

208. Tan A, Eskandar NG, Rao S, Prestidge CA. First in man bioavailability and tolerability studies of a silica–lipid hybrid (Lipoceramic) formulation: a Phase I study with ibuprofen. Drug Deliv Transl Res. 2014;4:212–21.

209. Barenholz YC. Doxil®—The first FDA-approved nano-drug: Lessons learned. J Controlled Release. 2012;160:117–34.

210. Cho H, Jeon SI, Ahn CH, Shim MK, Kim K. Emerging albumin-binding anticancer drugs for tumor-targeted drug delivery: current understandings and clinical translation. Pharmaceutics. 2022;14:728.

211. Lim SM, Kim TH, Jiang HH, Park CW, Lee S, Chen X, *et al.* Improved biological half-life and anti-tumor activity of TNF-related apoptosis-inducing ligand (TRAIL) using PEG-exposed nanoparticles. Biomaterials. 2011;32:3538–46.

212. He Q, Zhang Z, Gao F, Li Y, Shi J. *In vivo* biodistribution and urinary excretion of mesoporous silica nanoparticles: effects of particle size and PEGylation. Small. 2011;7:271–80.

213. Rodríguez F, Caruana P, De la Fuente N, Español P, Gamez M, Balart J, *et al.* Nano-based approved pharmaceuticals for cancer treatment: present and future challenges. Biomolecules. 2022;12:784.